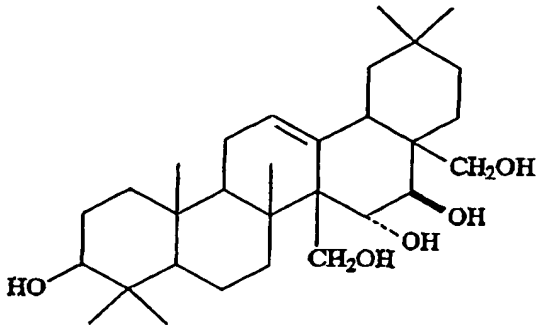

FIG 1. A_1-Barringenol

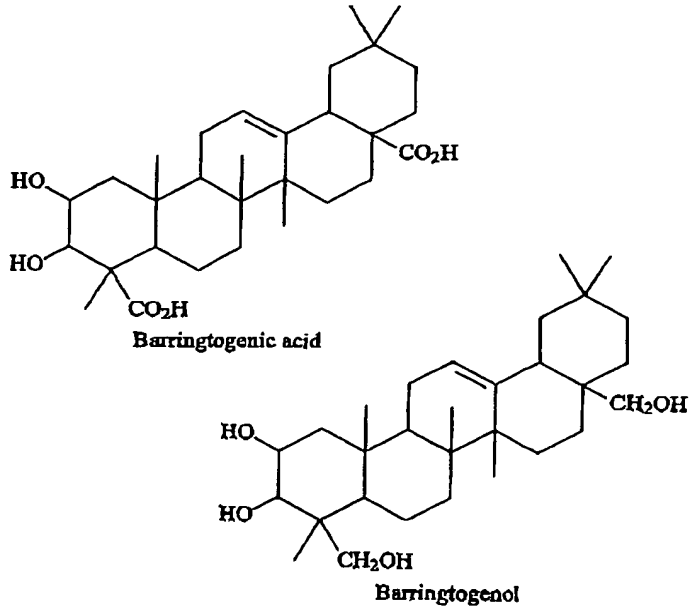

FIG 2. The structure of barringtogenic acid and barringtogenol

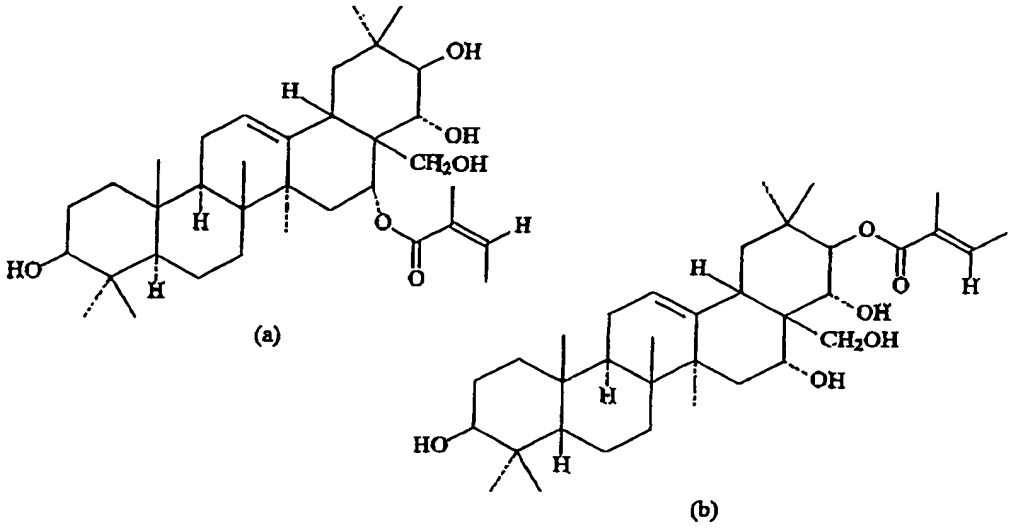

FIG 3 (a) Initial and (b) revised structures of barringtogenol B

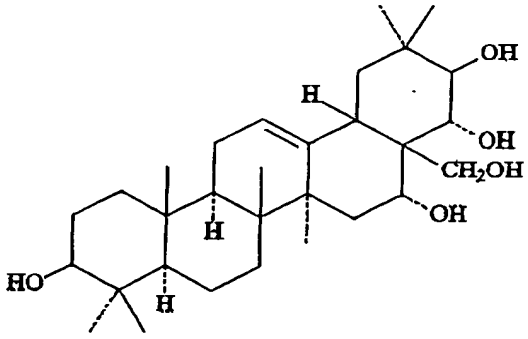

FIG 4 Barringtogenol C

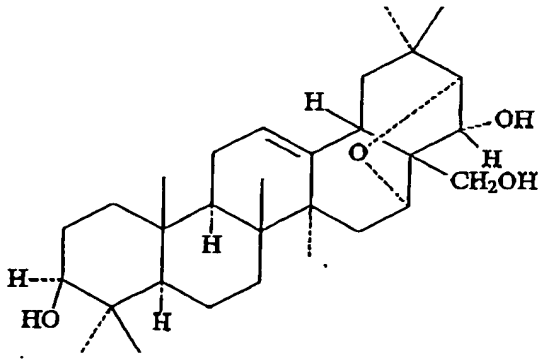

FIG 5 – Barringtogenol D

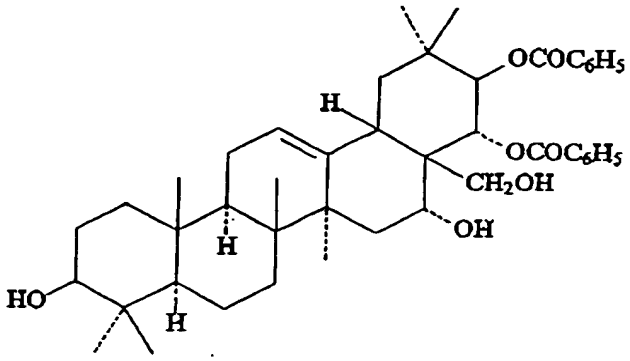

FIG 6 – Barringtogenol E

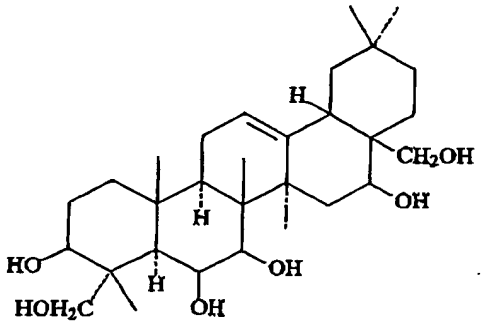

Tanginol

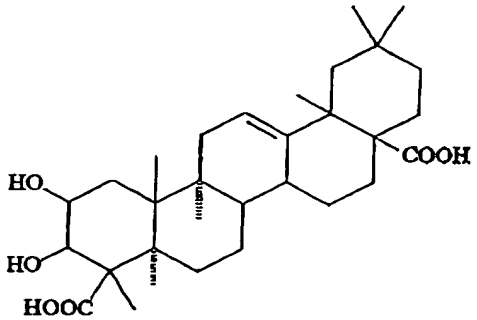

Barringtonic acid (third -OH unassigned)

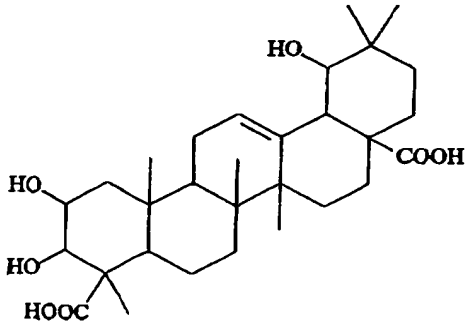

Acid A

FIG 7 – Compounds from *B. acutangula*

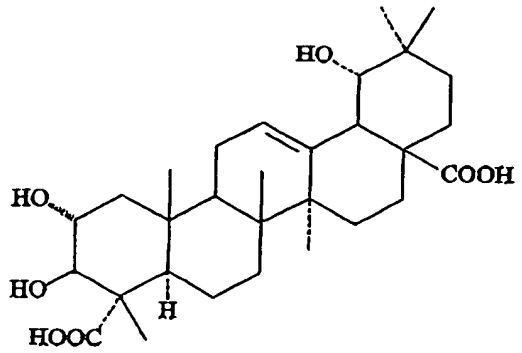

Barrinic acid

FIG 8. Barrinic acid

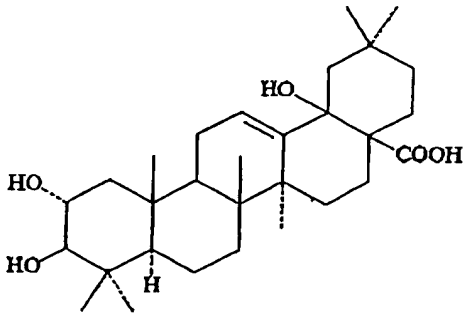

Acutangulic acid

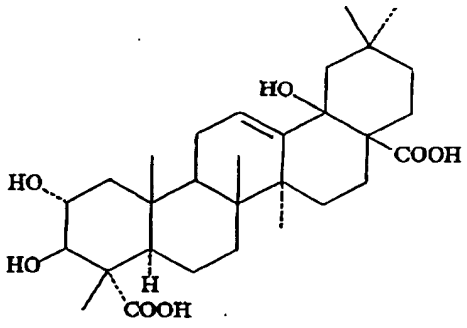

Tangulic acid

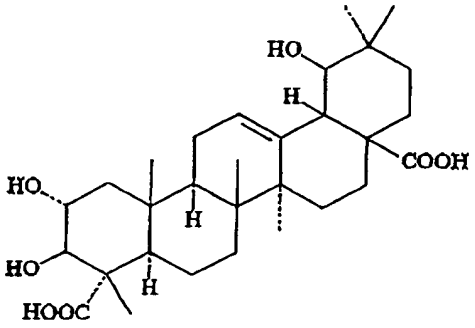

Barrigenic acid

FIG 9 – Compounds from B. acutangula

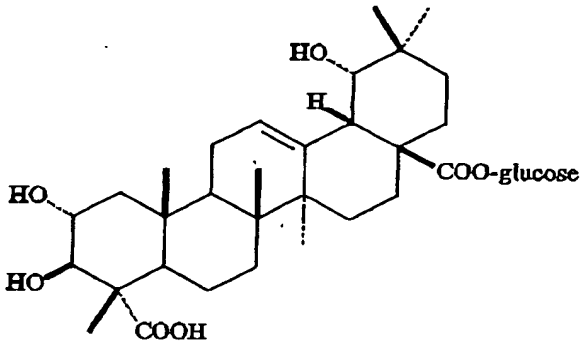

FIG 10 - 2α,3ß,19α-trihydroxy-olean-12-ene-dioic acid 28-O-ß-D-gluco-pyranoside from the seeds of B. acutangula

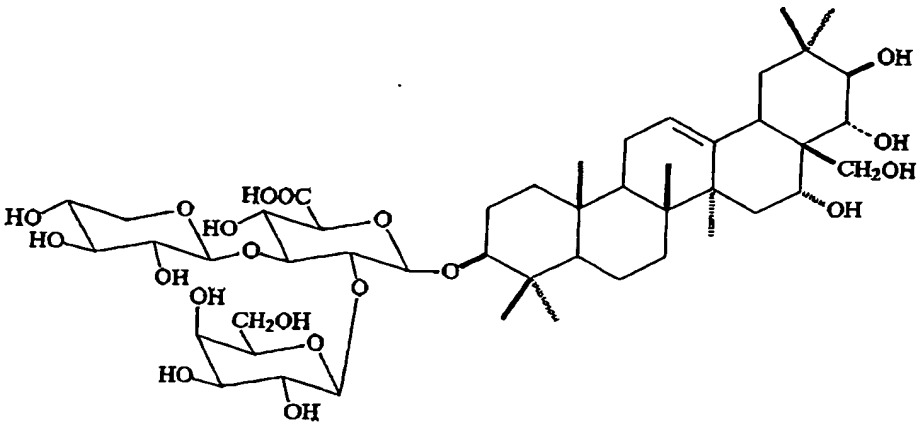

Barringtoside A = 3-*O*-β-D-xylopyranosyl(1→3)-[β-D-galactopyranosyl(1→2)]-β-D-glucuronopyranosyl barringtogenol C

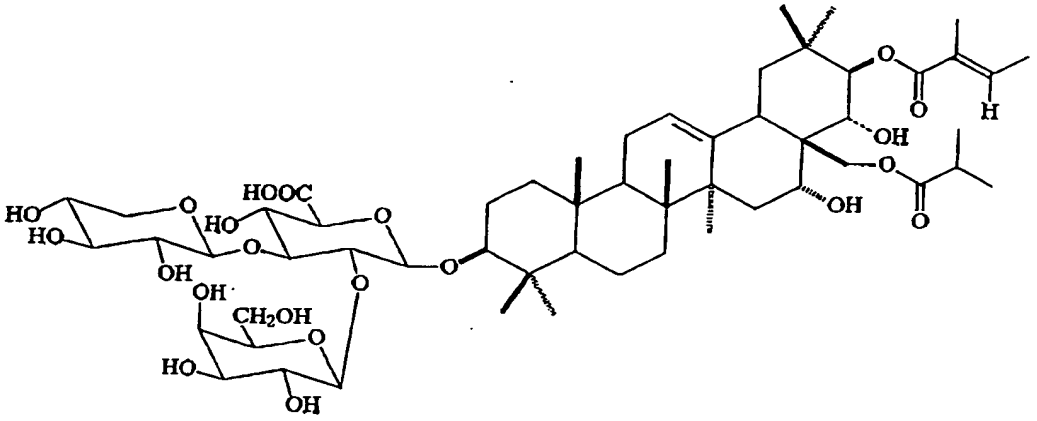

Barringtoside B = 3-*O*- β-D-xylopyranosyl(1→3)-[β-D-galactopyranosyl(1→2)]-β-D-glucuronopyranosyl -21-*O*-tigloyl-28-*O*-isobutyryl barringtogenol C

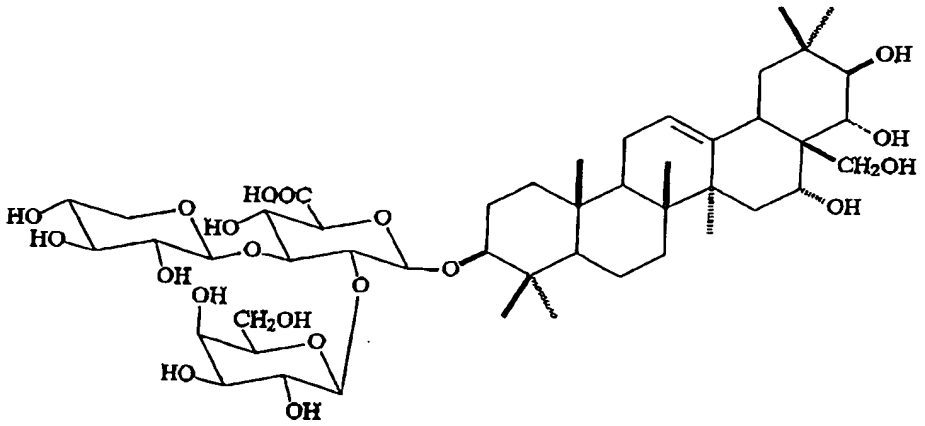

Barringtoside C = 3-*O*-α-L-arabinopyranosyl(1→3)-[β-D-galactopyranosyl(1→2)]-β-D-glucuronopyranosyl barringtogenol C

FIG 11

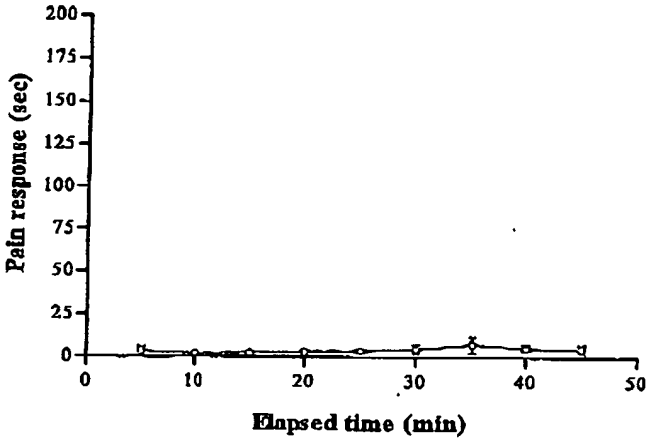

FIG 12 - Normal grooming response ($\bar{x}$ ± S.E.; n = 6).

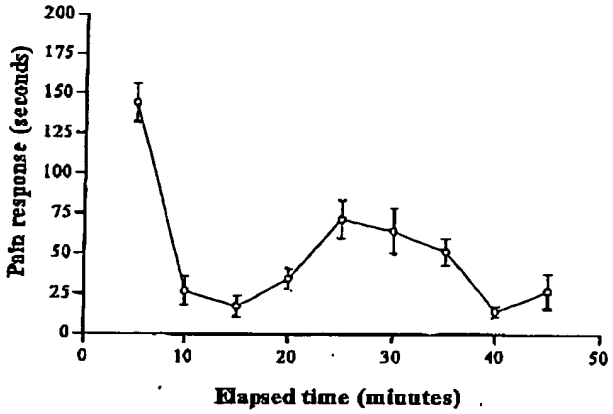

FIG 13 - Control values ($\bar{x}$ ± S.E.; n = 18).

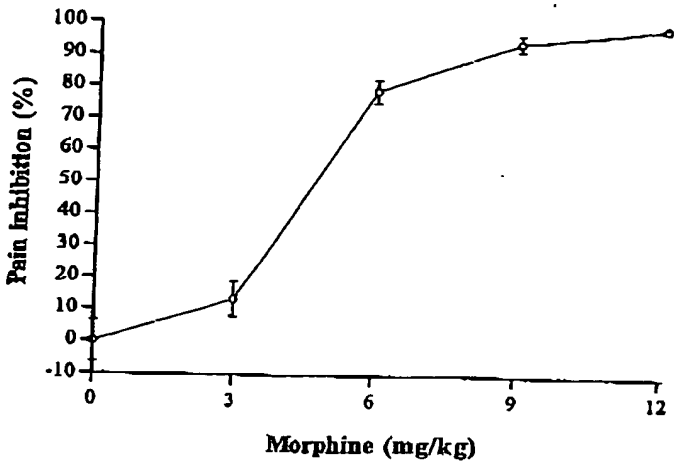

FIG 14 - Dose response curve for morphine ($\bar{x}$ ± S.E.; n = 6(min)).

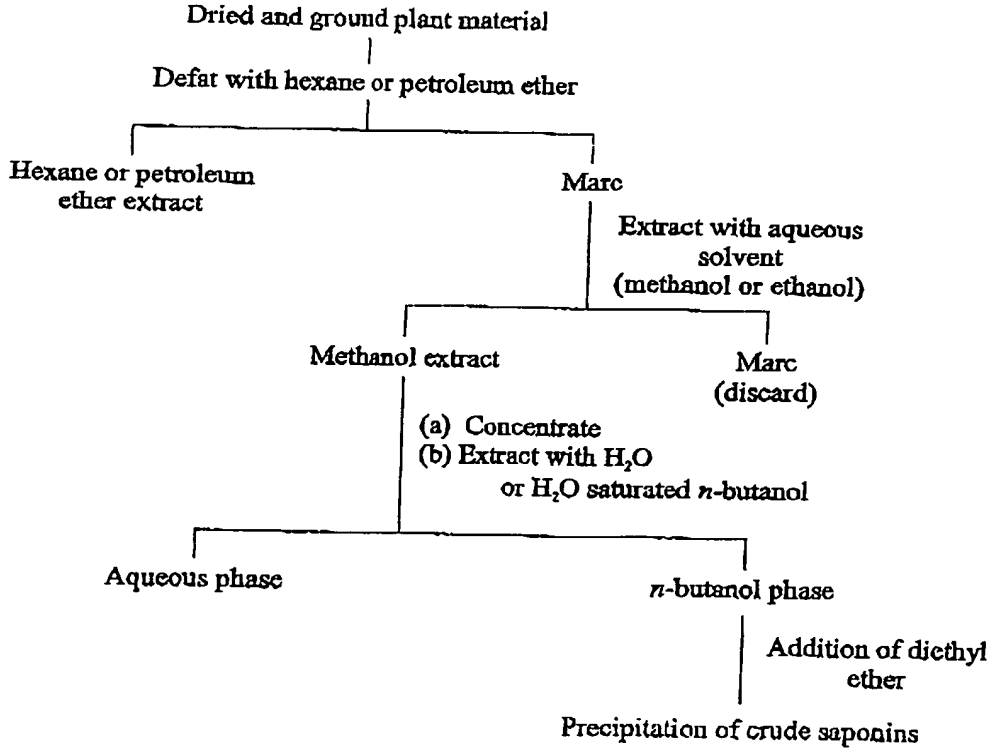

FIG 15 - Schematic for the preparation of crude saponin mixtures.

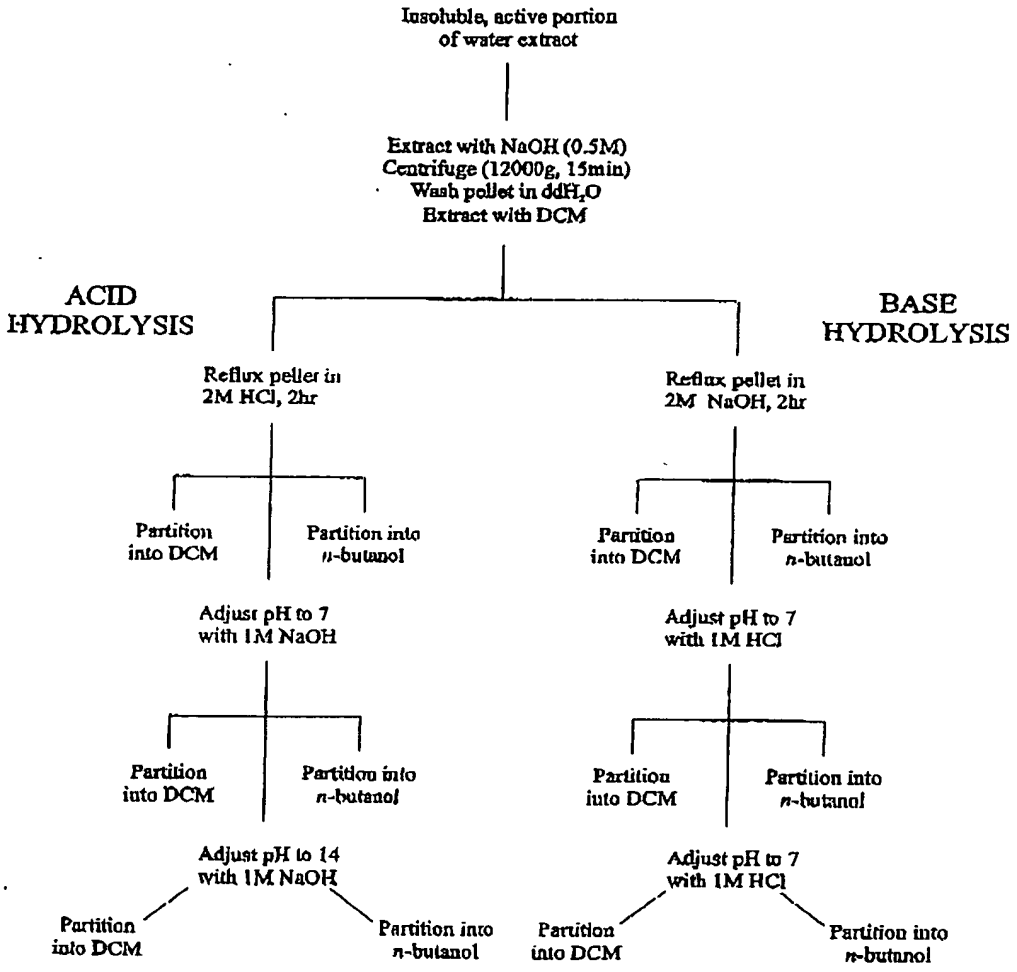

FIG 16 - Acid and base hydrolysis scheme.

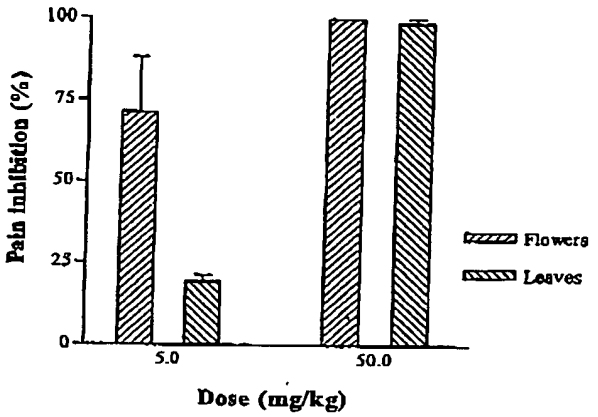

FIG 17 - Analgesic activity of water extract of flowers and leaves of *B. acutangula* ($\bar{x} \pm$ SE, n=2).

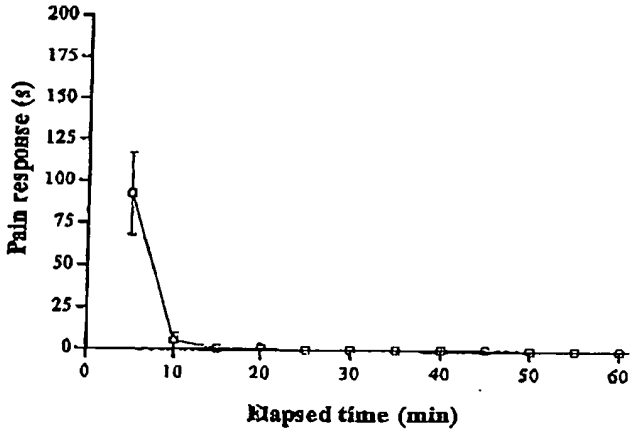

FIG 18 - Analgesic activity of crude water extract ($\bar{x} \pm$ SE, n=5).

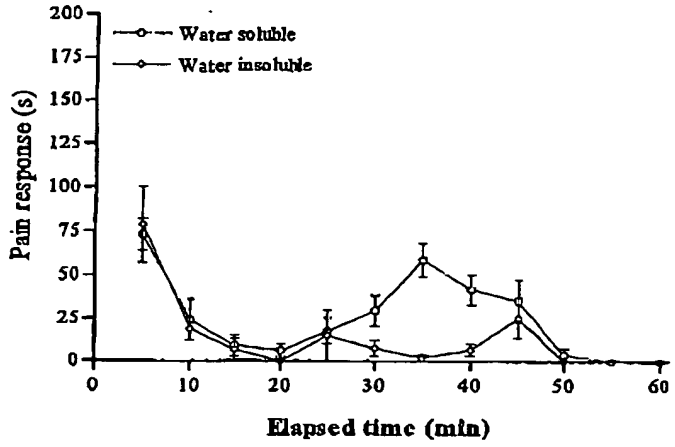

FIG 19 - Analgesic activity of crude water soluble (n=9) and insoluble (n=4) portions of the water extract ($\bar{x}$ ± SE).

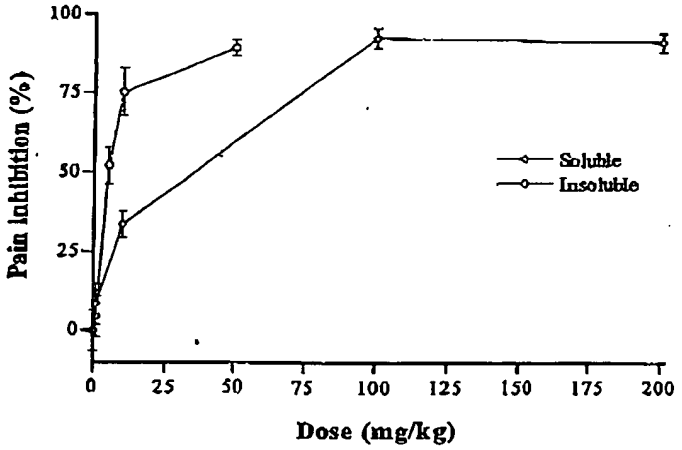

FIG 20 - Dose response curves for water extract ($\bar{x}$ ± SE, n=4).

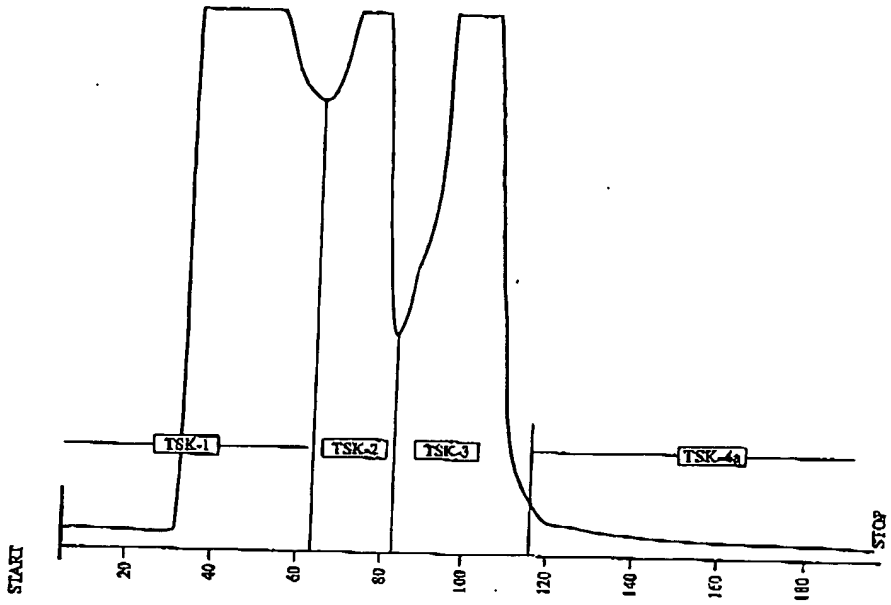

FIG 21 - Preparative gel permeation column.

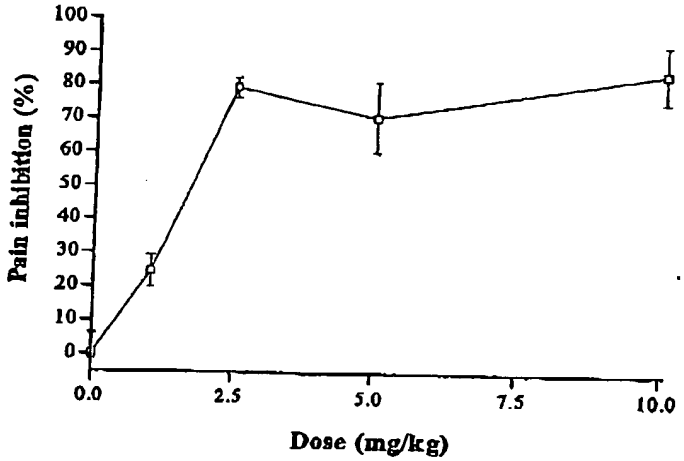

FIG 22 - Dose response curve for TSK-4a ($\bar{x} \pm$ SE, n=3).

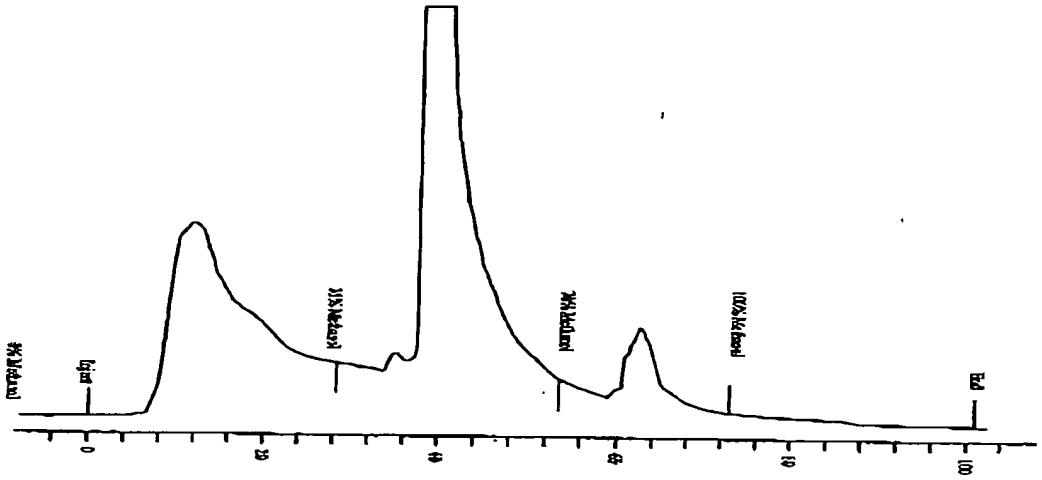

FIG 23 - C18 separation of TSK-4a.

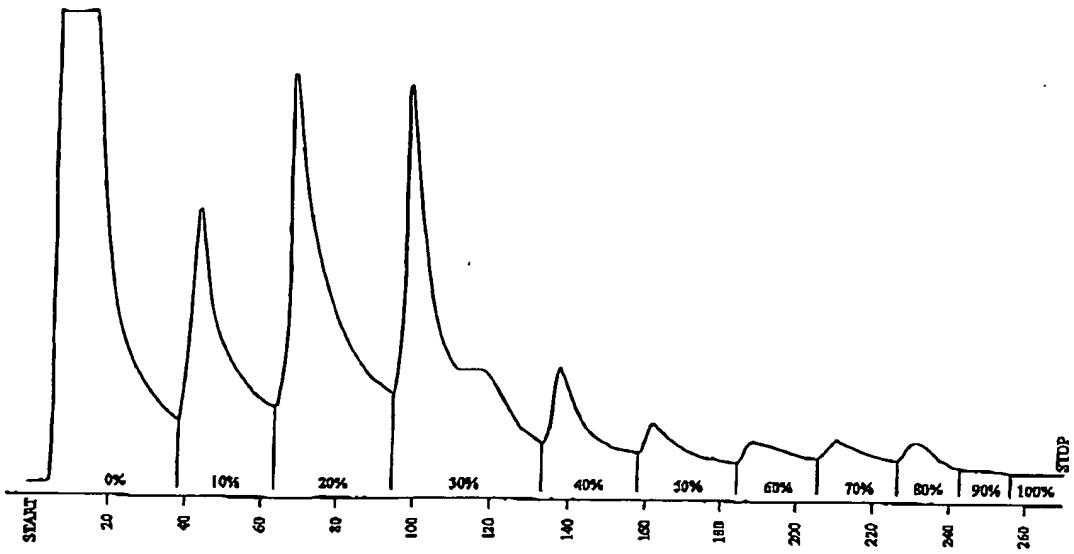

FIG 24 - C18 preparative separation of TSK-4a.

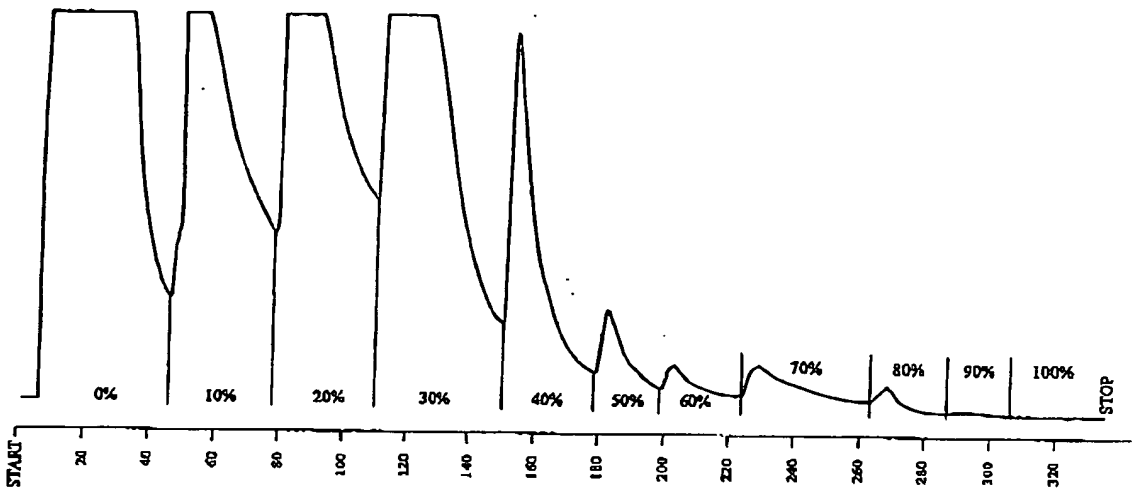

FIG 25 - Preparative C18 chromatogram of H_2O extract

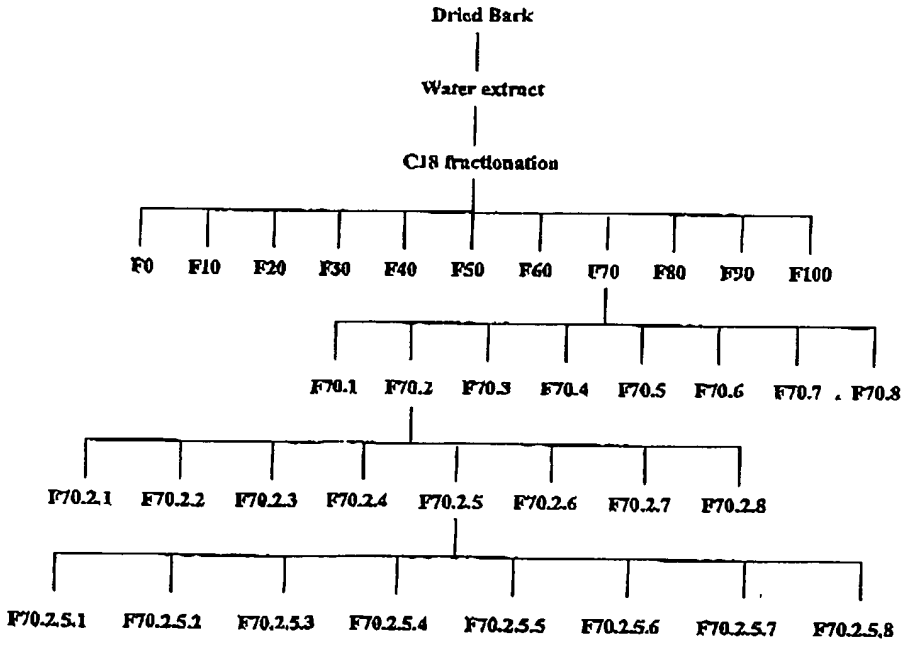

FIG 26 - Outline of numbering system compound F70.2.5.2.

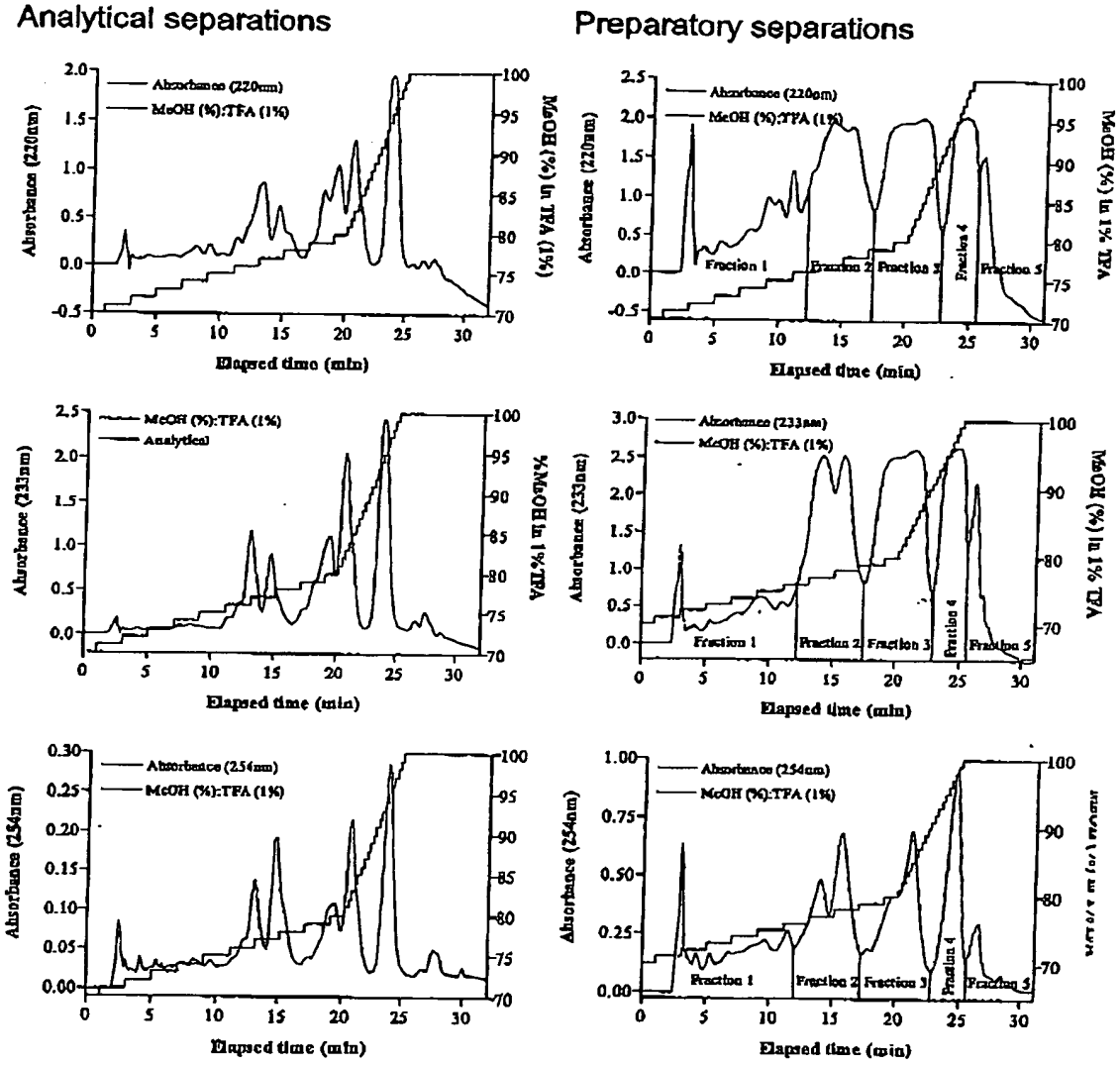

FIG 27 - Separation of fraction eluting at 70% MeOH (F70).

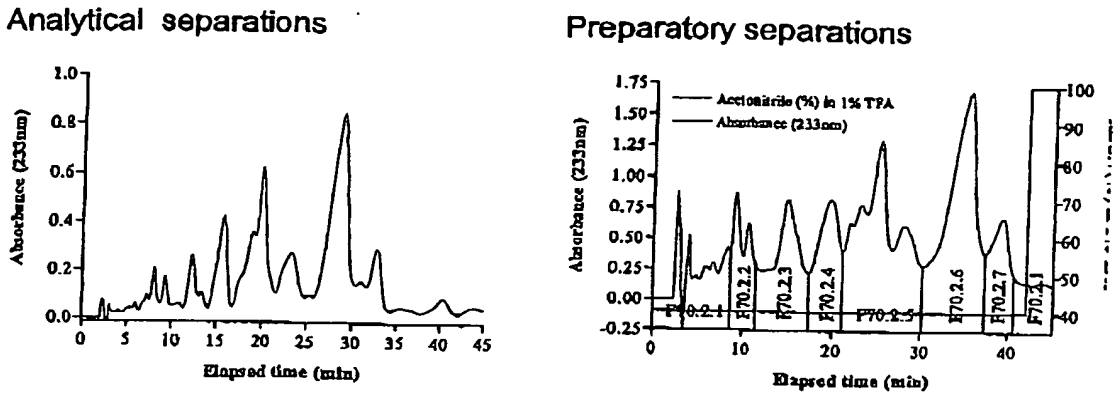

FIG 28 - Separation of fraction F70.2 (40%MeCN in 1%TFA).

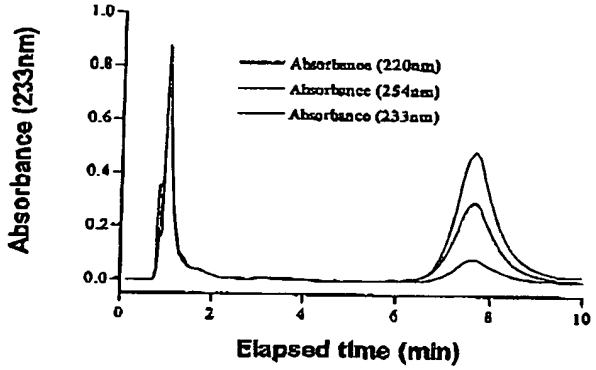

FIG 29 - Chromatogram of F70.2.6.

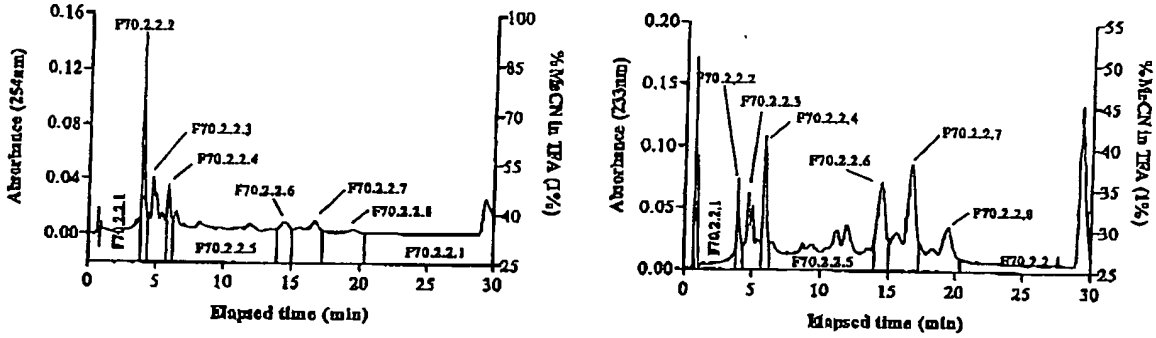

FIG 30 - Separation of fraction F70.2.2 at 254nm (left) and 233nm (right).

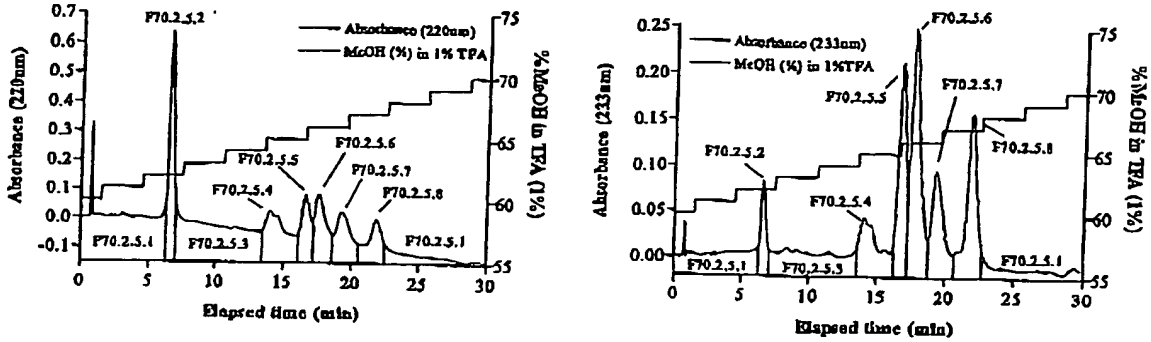

FIG 31 - Separation of fraction F70.2.5 at 220nm (left) and 233nm (right).

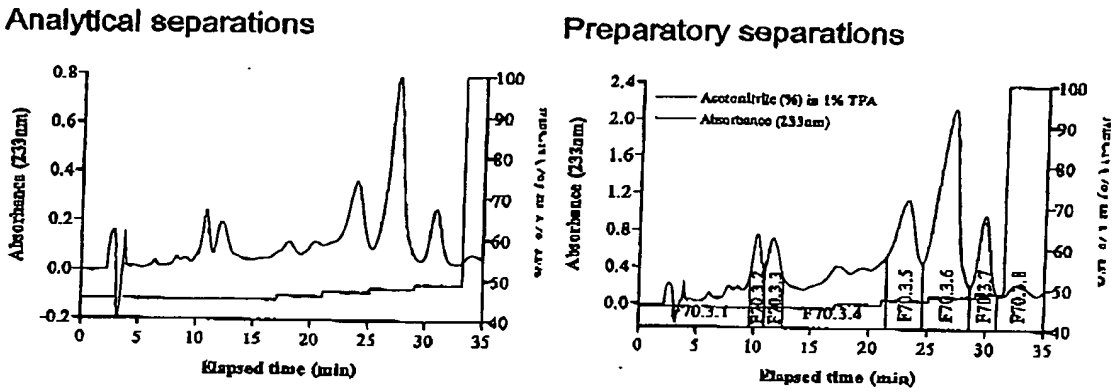

FIG 32 - Separation of fraction F70.3.

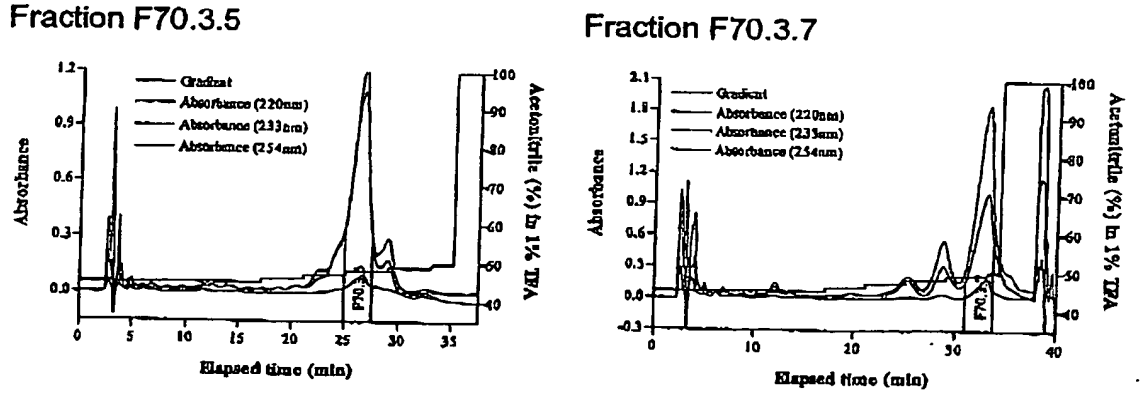

FIG 33 - Chromatograms of F70.3.5 and F70.3.7.

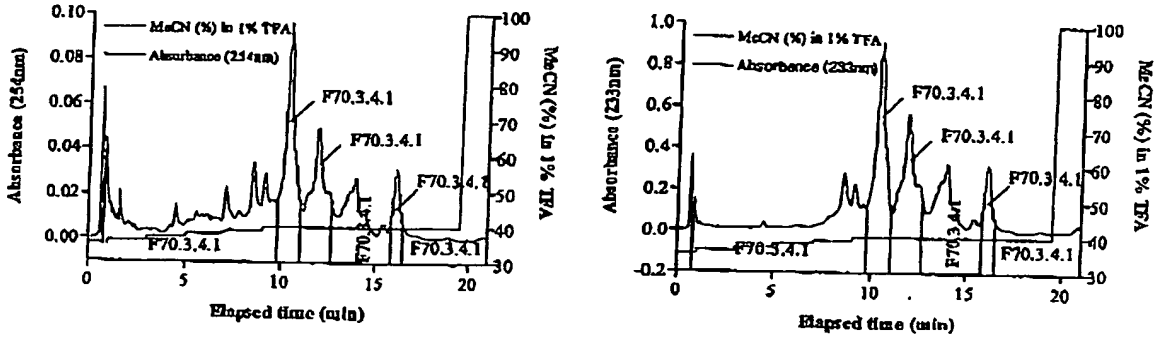

FIG 34 - Analytical separation of fraction F70.3.4 at 254 and 233nm.

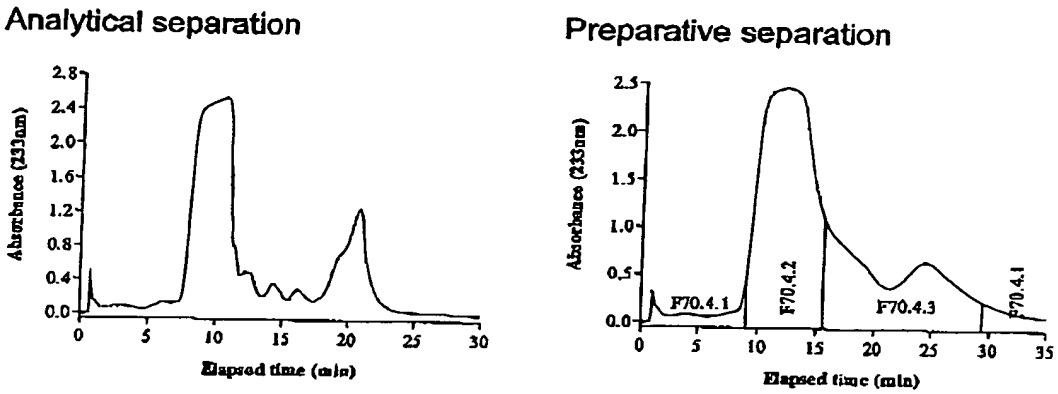

FIG 35 - Separation of F70.4.

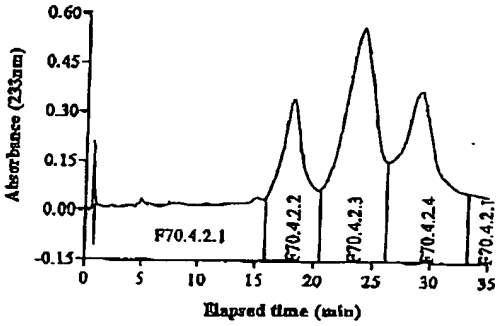

FIG 36 - Separation of F70.4.2.

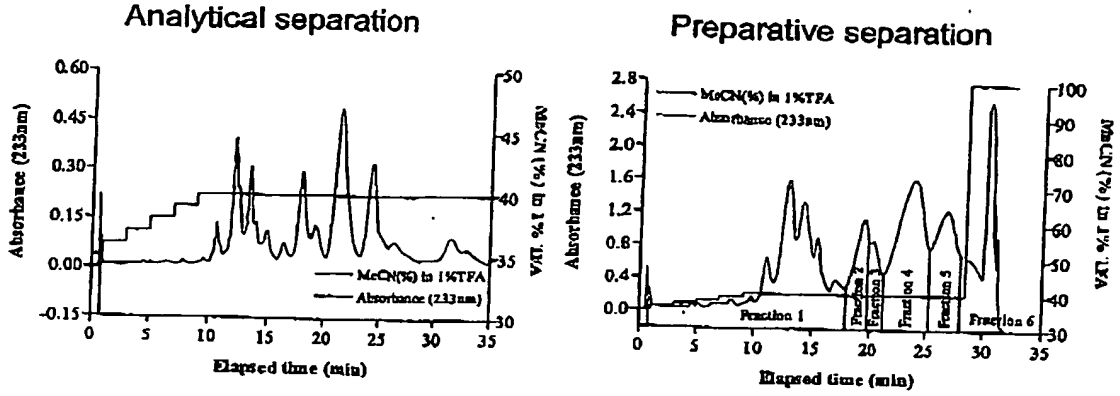

FIG 37 – Analytical separation (left) and preparative separation (right) of F70.4.3.

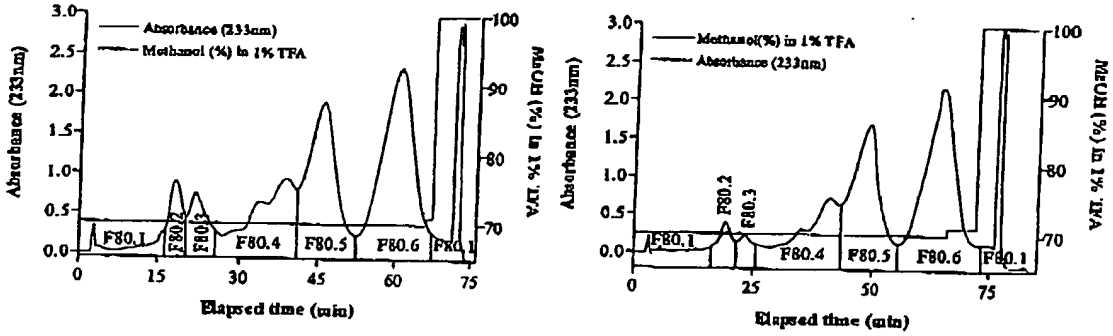

FIG 38 - Preparative chromatograms showing loss of peaks F80.2 & F80.3.

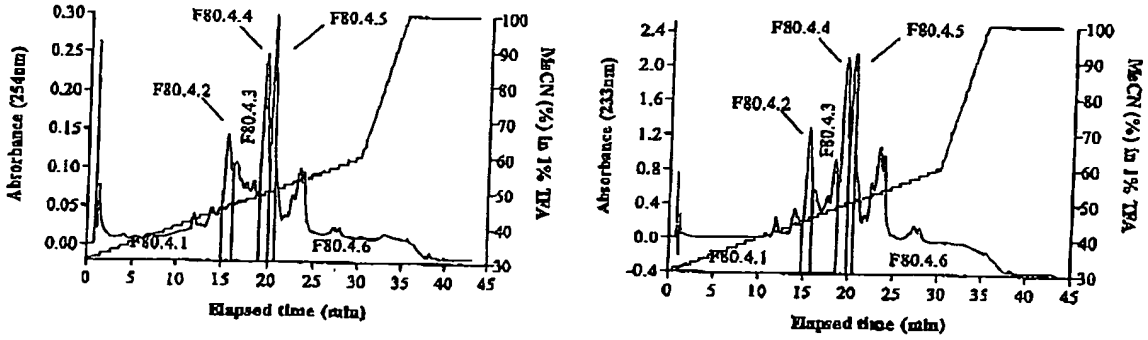

FIG 39 - Preparative chromatograms of F80.4.

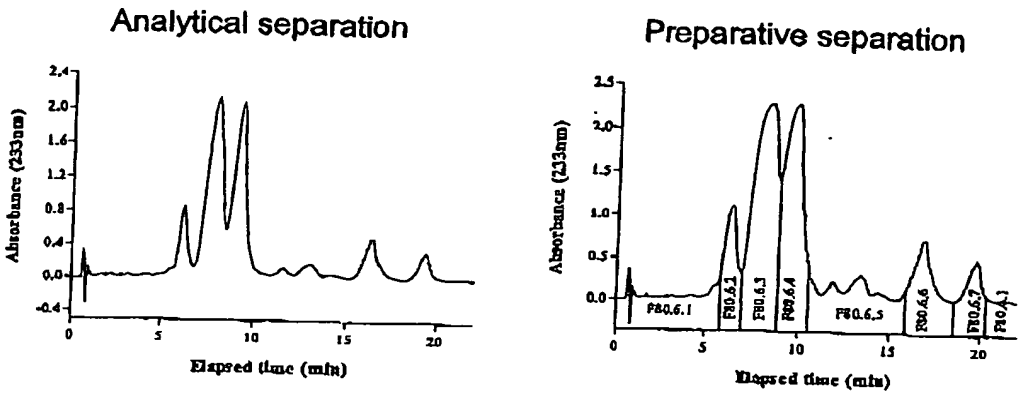

FIG 40 - Separation of fraction F80.6 using a phenyl reverse phase column with the analytical separation (left) and the preparative separation (right).

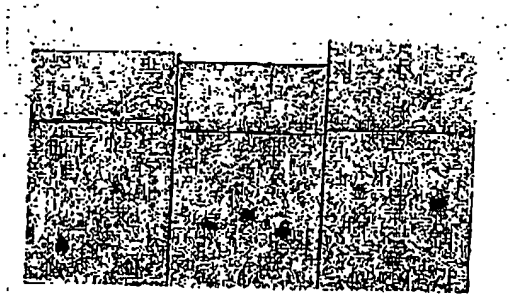

FIG 41 - Standard sugars used for TLC

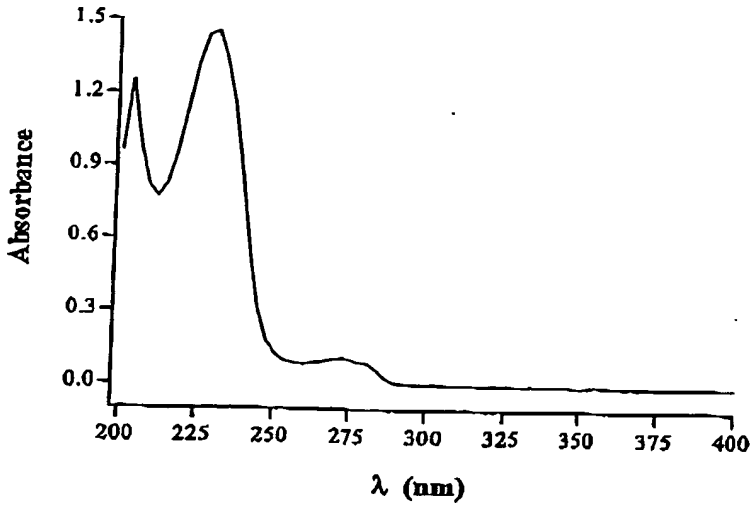

FIG 42 - UV spectrum of F70.3.6

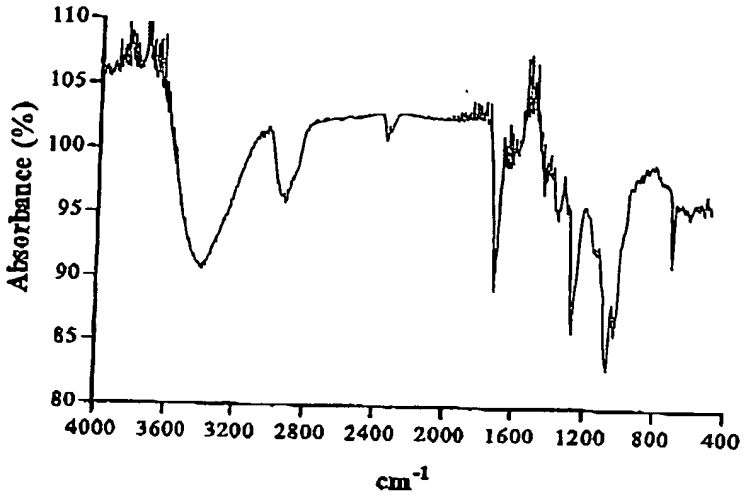

FIG 43 - FTIR spectrum of F70.3.6

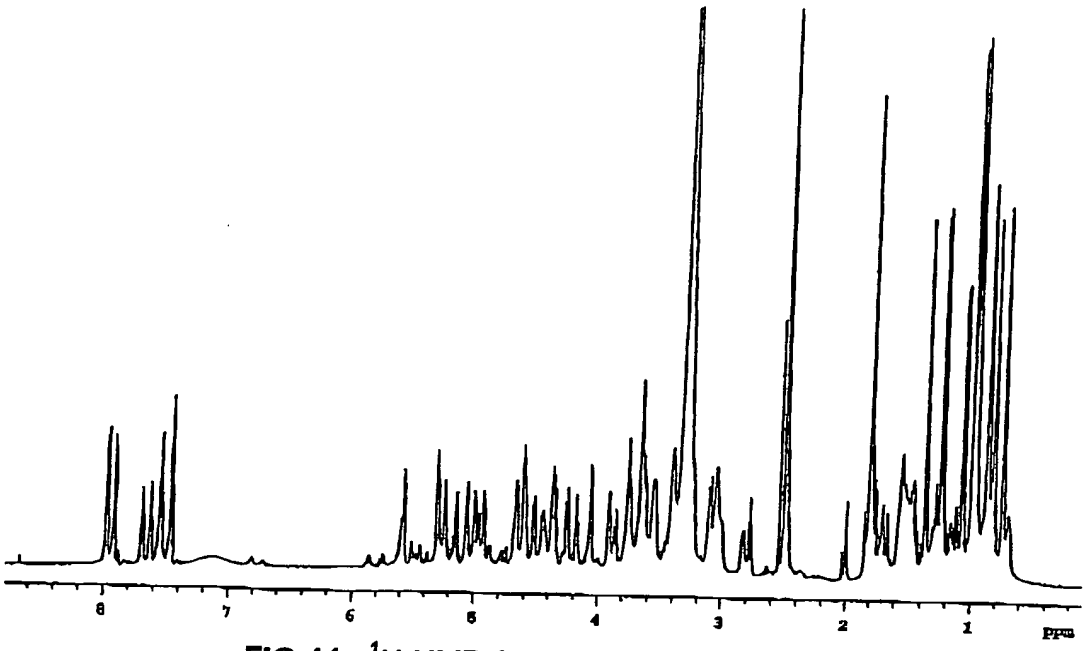

FIG 44 - ^{1}H-NMR for compound F70.3.6

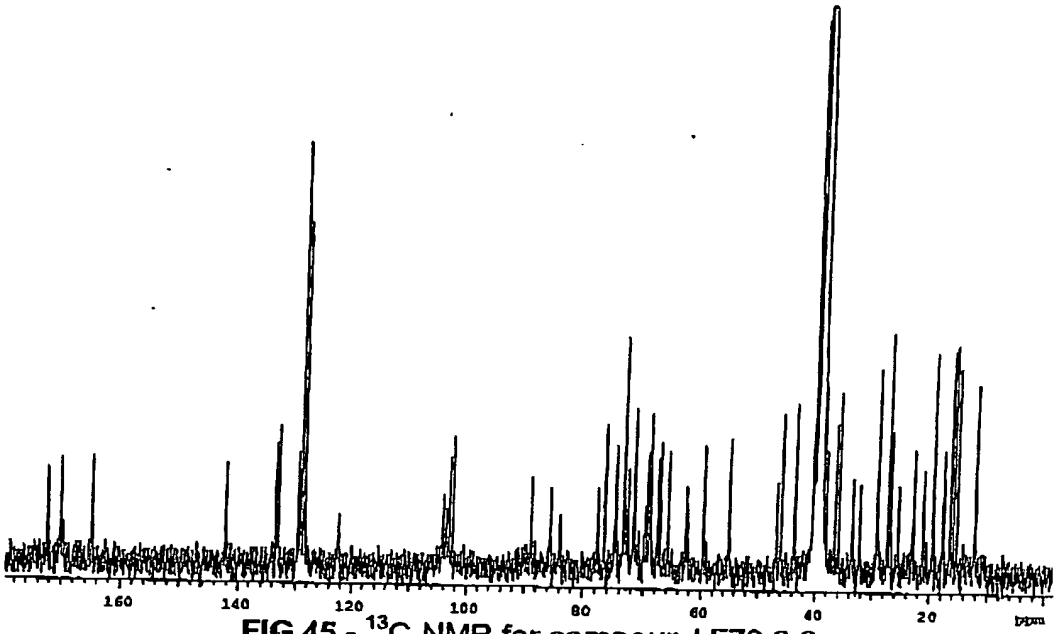

FIG 45 - ^{13}C-NMR for compound F70.3.6

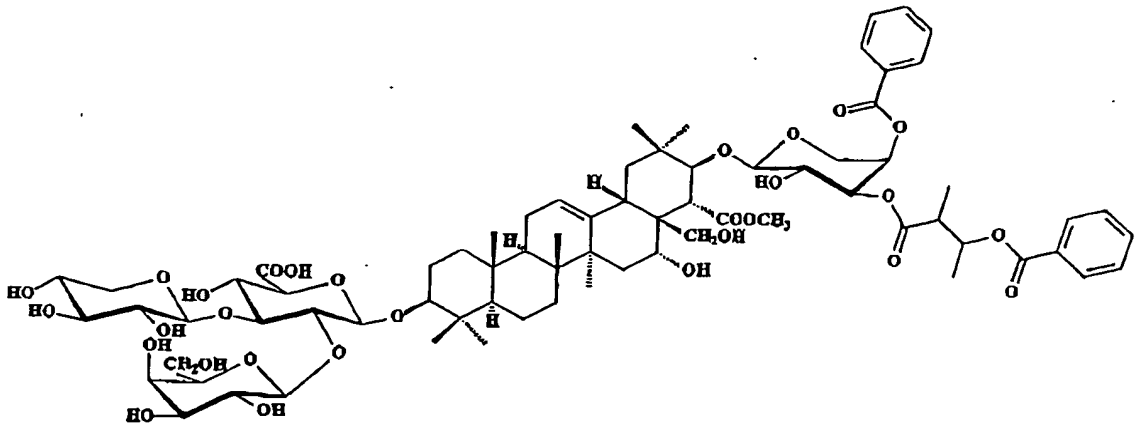

FIG 46 - The complete assignment of F70.3.6 *(3-O-ß-D-xylopyranosyl(1? 3)-[ß-D-galactopyranosyl(1? 2)]-ß-D-glucuronopyranosyl-21-O-[3-(3-benzoyl-2-methylbutanoyl)-4-benzoyl-α-L-arabinopyranosyl]-22-O-acetyl barringtogenol C)*

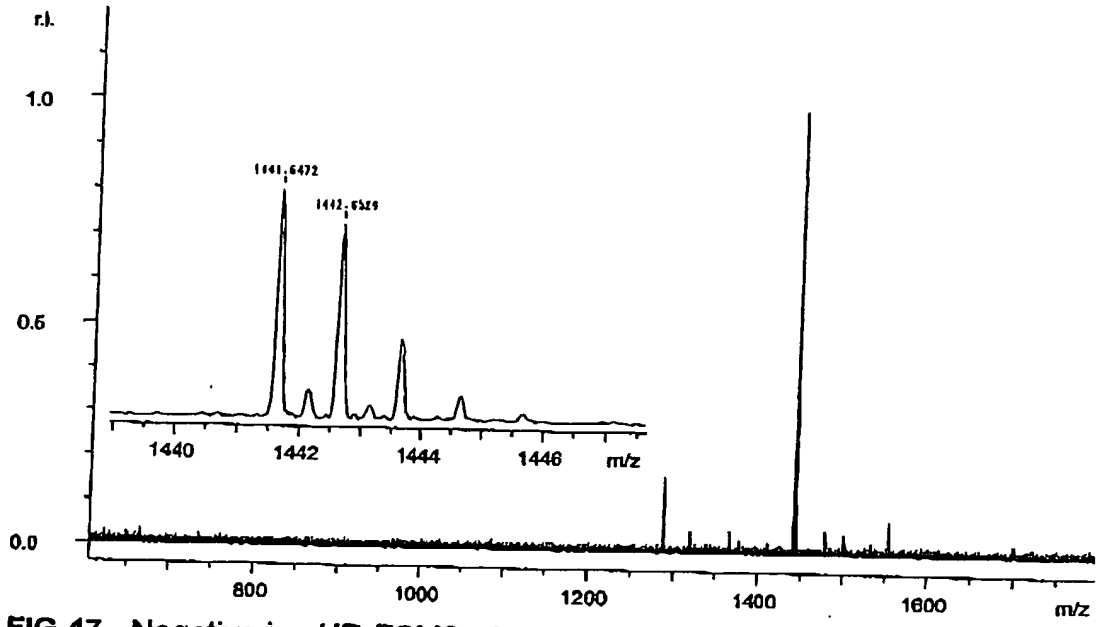

FIG 47 - Negative ion HR-ESMS of F70.3.6 (insets show detail of molecular ion)

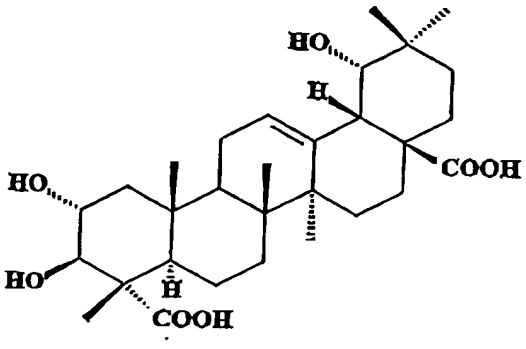

FIG 48 - Compound F70.2.5.2
(2α, 3ß, 19α -trihydroxy-olean-12-ene-23, 28-dioic acid)

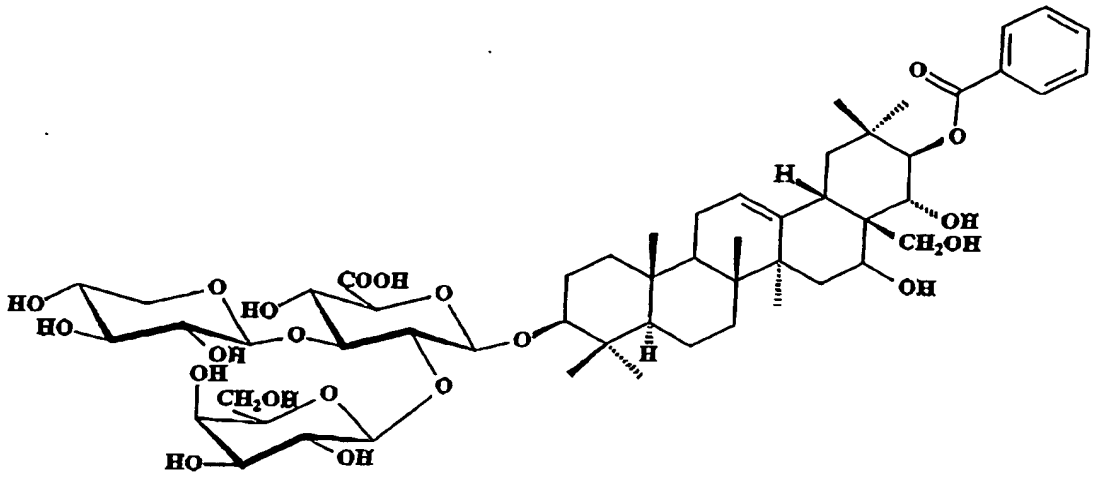

2

FIG 49 - Compound F70.2.3.
(3-O-ß-D-xylopyranosyl(1→3)-[ß-D-galactopyranosyl(1→2)]-ß-D-glucuronopyranosyl-21-O-benzoyl barringtogenol C)

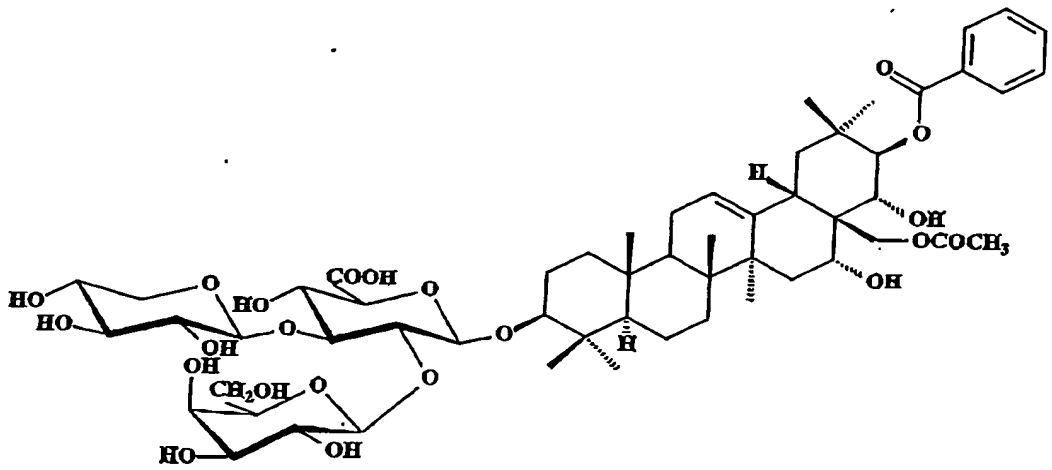

FIG 50 - Compound F70.3.2
3-O-ß-D-xylopyranosyl(1→3)-[ß-D-galactopyranosyl(1→2)]-ß-D-glucuronopyranosyl-21-O-benzoyl-28-O-acetyl barringtogenol C)

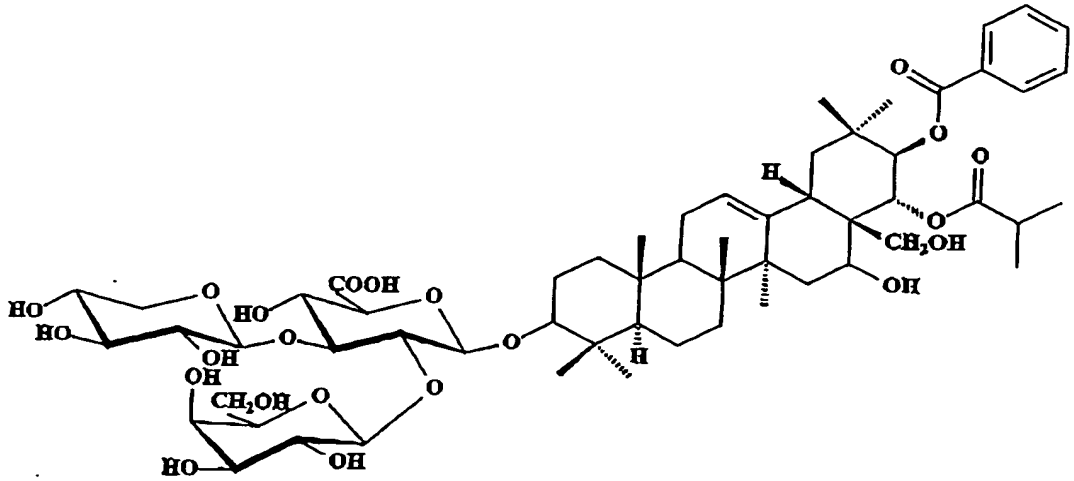

FIG 51 - Compound F70.3.4.2
(3-O-ß-D-xylopyranosyl(1→3)-[ß-D-galactopyranosyl(1→2)]-ß-D-glucuronopyranosyl-21-O-benzoyl-22-O-isobutyryl barringtogenol C)

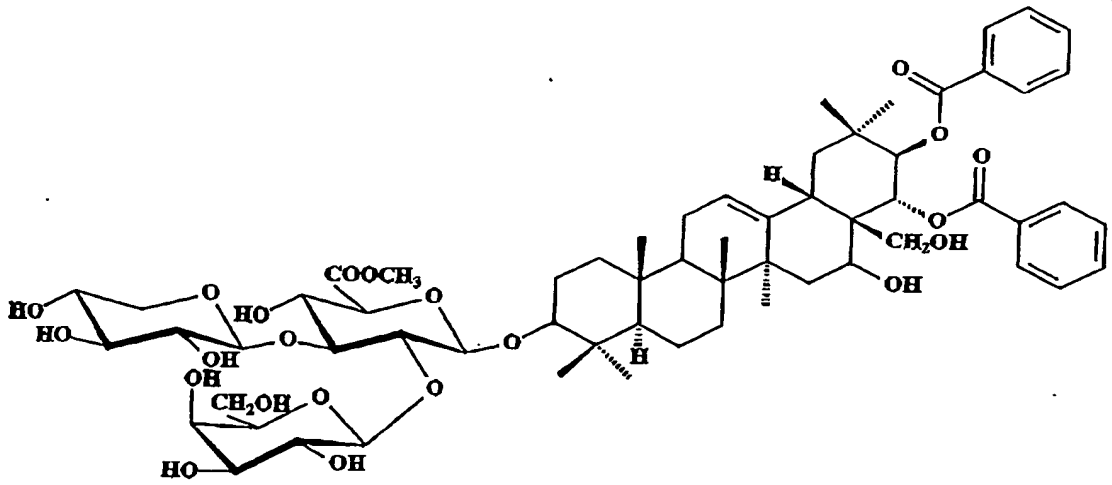

FIG 52 - Compounds F70.4.3.5.2/F80.6.7
(3-O-ß-D-xylopyranosyl(1→3)-[ß-D-galactopyranosyl(1→2)]-ß-D-methylglucuronopyranosyl-21,22-O-dibenzoyl barringtogenol C)

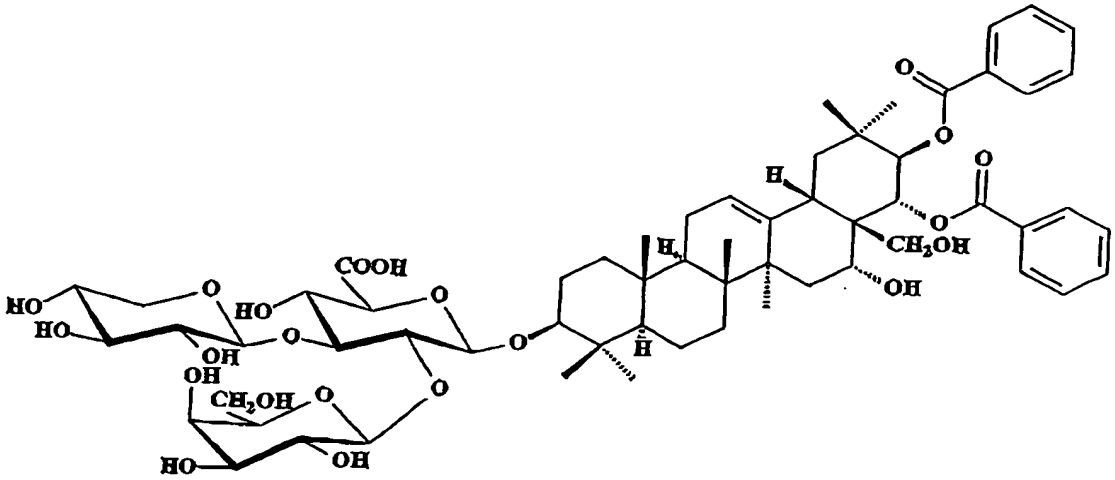

FIG 53 - Compound F80.6.4/F70.4.2.4.2
(3-O-ß-D-xylopyranosyl(1→3)-[ß-D-galactopyranosyl(1→2)]-ß-D-glucuronopyranosyl-21, 22-O-dibenzoyl barringtogenol C

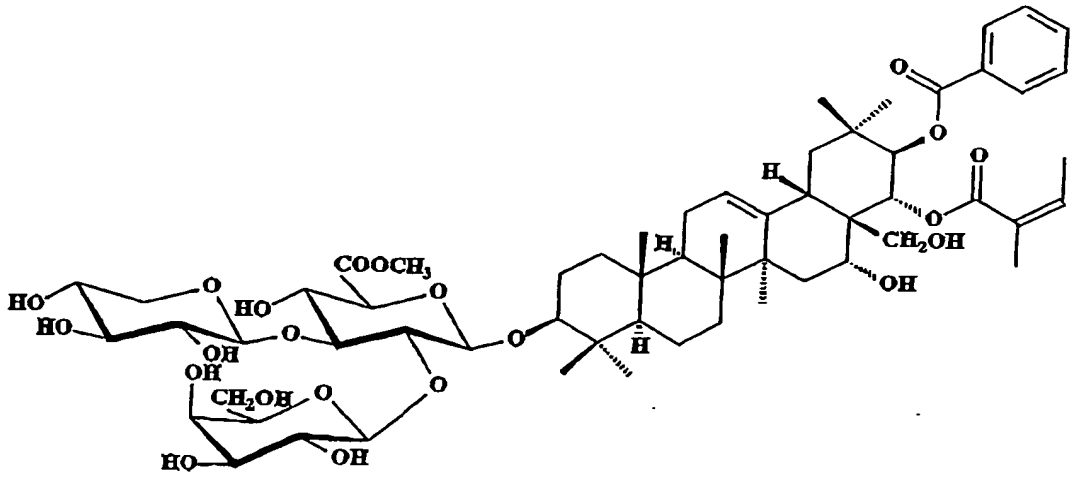

FIG 54 - Compound F70.4.3.4.2/F80.6.6
(3-O-ß-D-xylopyranosyl(1→3)-[ß-D-galactopyranosyl(1→2)]-ß-D-methylglucuronopyranosyl-21-O-benzoyl-22-O-tigloyl barringtogenol C)

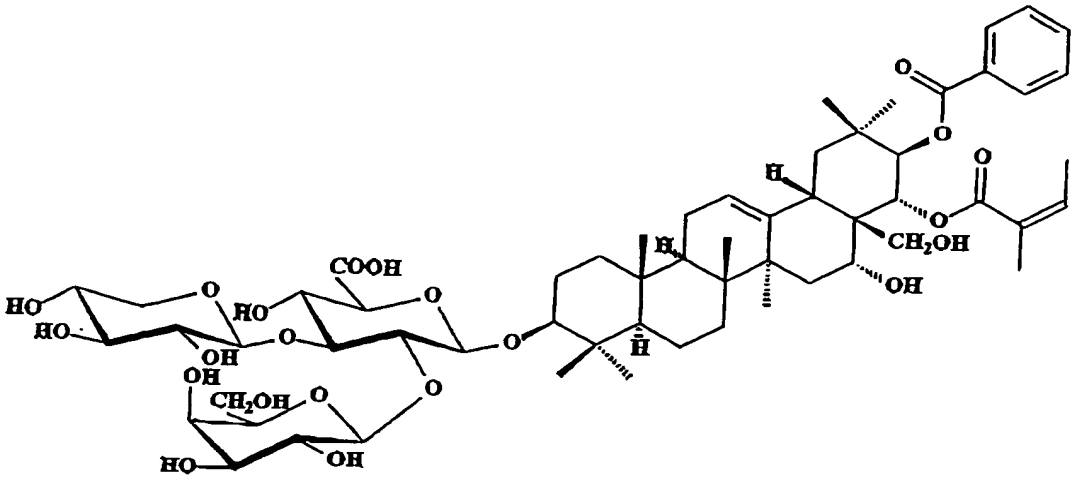

FIG 55 - Compound F70.4.2.3/F80.6.3
(3-O-ß-D-xylopyranosyl(1→3)-[ß-D-galactopyranosyl(1→2)]-ß-D-glucuronopyranosyl-21-O-benzoyl-22-O-tigloyl barringtogenol C)

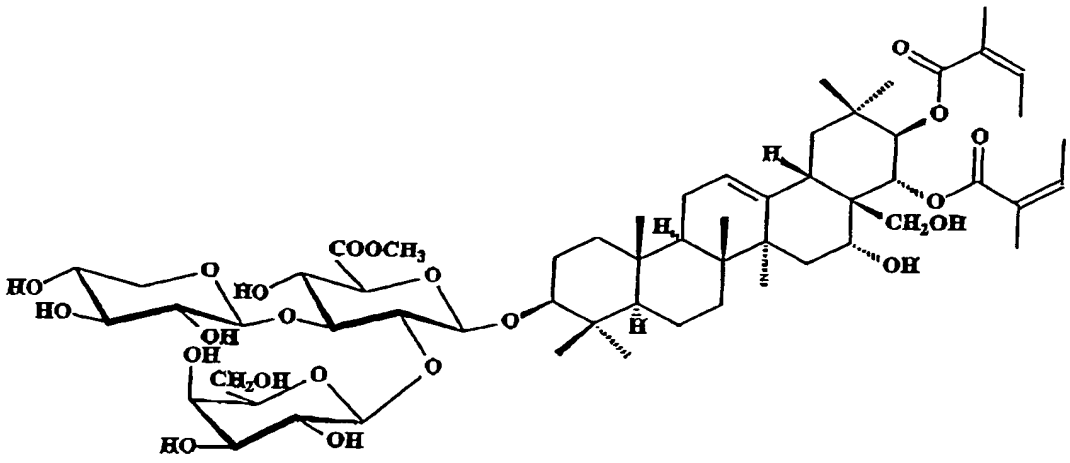

FIG 56 - Compound F70.4.3.2.2
(3-O-ß-D-xylopyranosyl(1→3)-[ß-D-galactopyranosyl(1→2)]-ß-D-methylglucuronopyranosyl-21,22-O-tigloyl barringtogenol C)

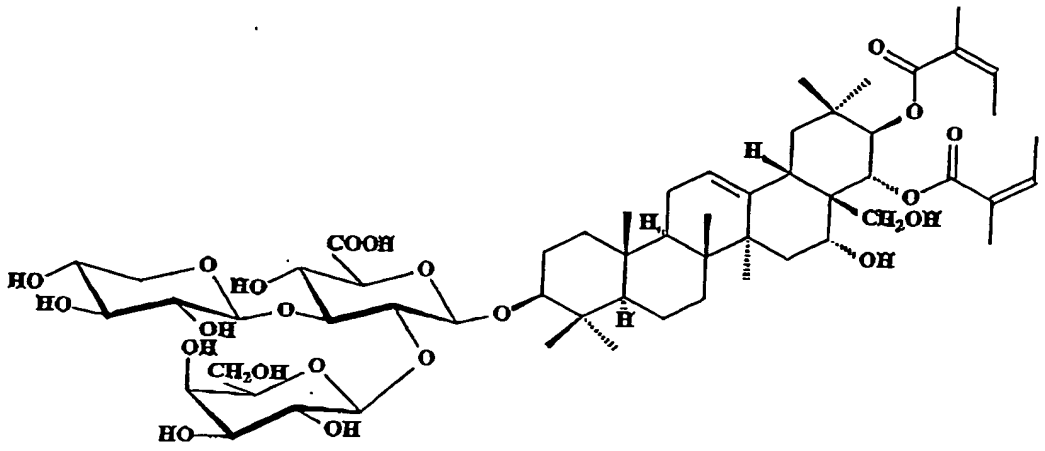

FIG 57 - Compound F80.6.2
(3-O-ß-D-xylopyranosyl(1→3)-[ß-D-galactopyranosyl(1→2)]-ß-D-glucuronopyranosyl-21,22-O-tigloyl barringtogenol C)

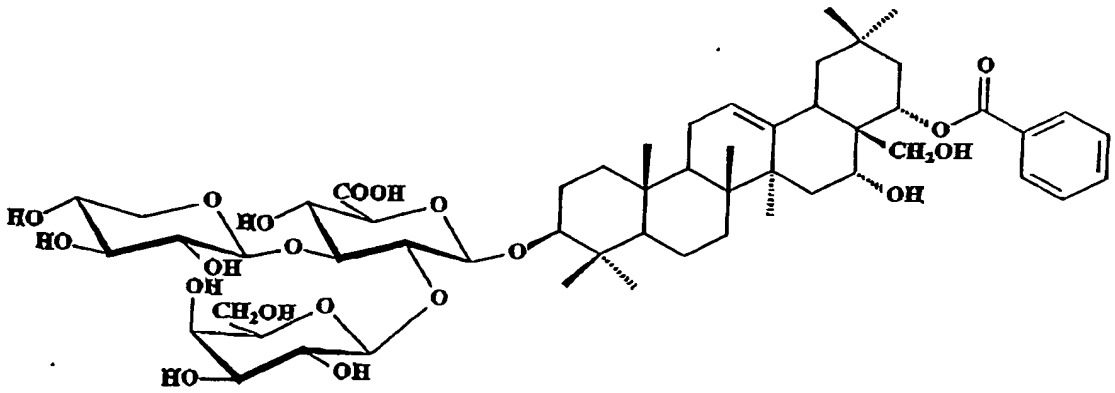

FIG 58 - Compound F70.3.3.2.2b
(3-O-ß-D-xylopyranosyl(1→3)-[ß-D-galactopyranosyl(1→2)]-ß-D-glucuronopyranosyl-22-O-benzoyl barringtogenol C)

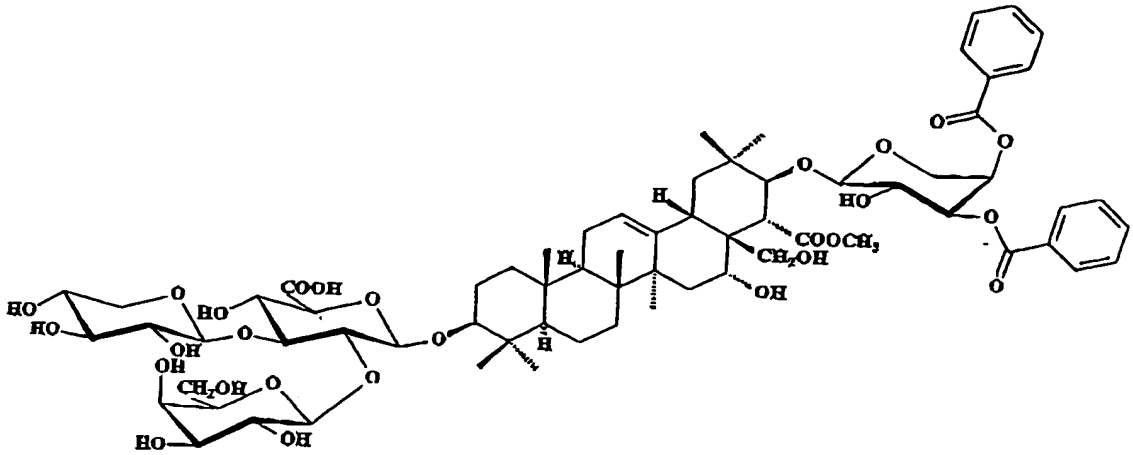

FIG 59 - Compound F70.2.6.2
(3-O-ß-D-xylopyranosyl(1→3)-[ß-D-galactopyranosyl(1→2)]-ß-D-glucuronopyranosyl-21-O-[3,4-dibenzoyl-∀-L-arabinopyranosyl]-22-O-acetyl barringtogenol C)

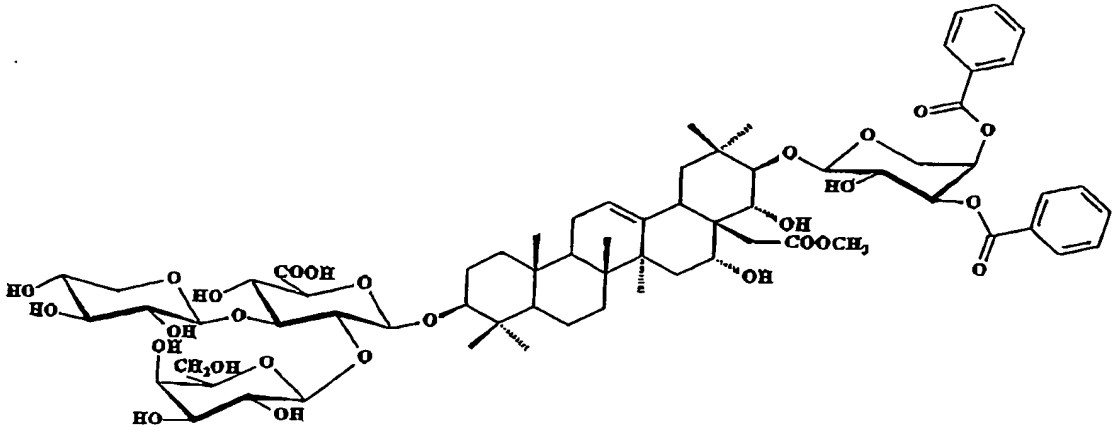

FIG 60 - Compound F70.3.4.5
(3-O-ß-D-xylopyranosyl(1→3)-[ß-D-galactopyranosyl(1→2)]-ß-D-glucuronopyranosyl-21-O-[3,4-dibenzoyl-α-L-arabinopyranosyl]-28-O-acetyl barringtogenol C)

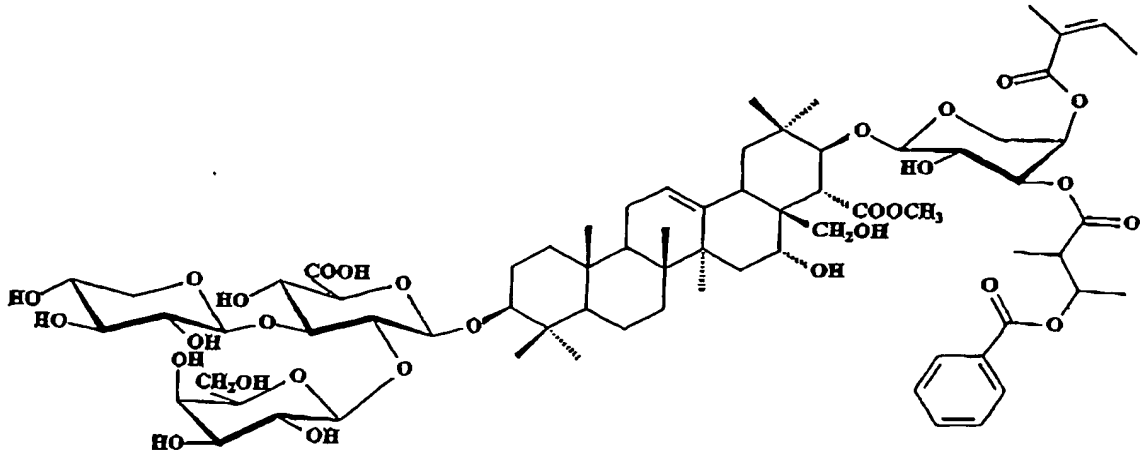

FIG 61 - Compound F70.3.5a

(3-O-ß-D-xylopyranosyl(1→3)-[ß-D-galactopyranosyl(1→2)]-ß-D-glucuronopyranosyl-21-O-[3-(3-benzoyl-2-methylbutyryl)-4-tigloyl-α-L-arabinopyranosyl]-22-O-acetyl barringtogenol C)

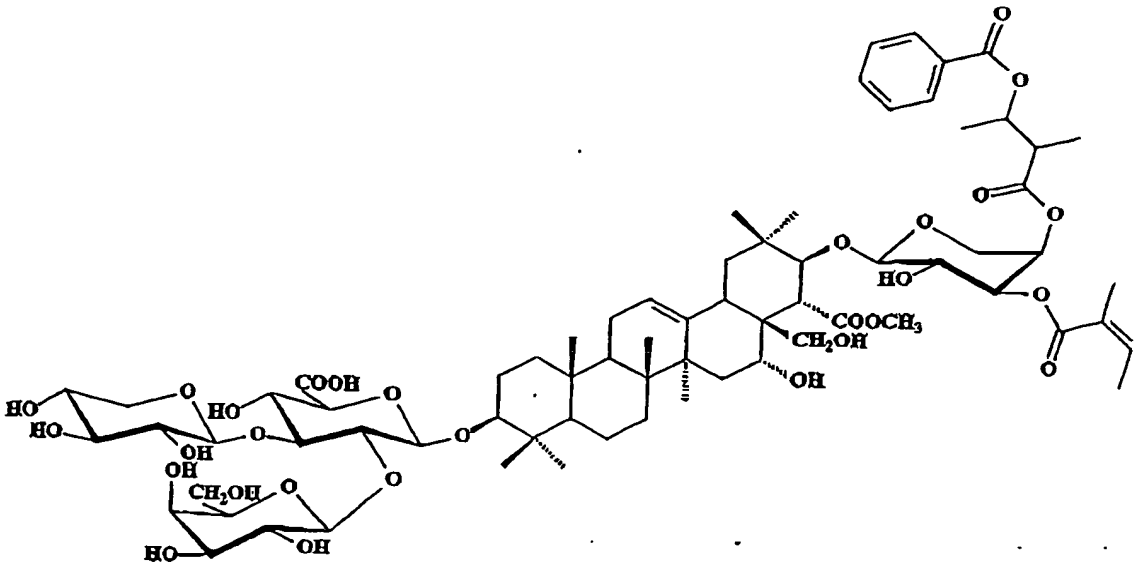

FIG 62 - Compound F70.3.5b

(3-O-ß-D-xylopyranosyl(1→3)-[ß-D-galactopyranosyl(1→2)]-ß-D-glucuronopyranosyl-21-O-[3-tigloyl-4-(3-benzoyl-2-methylbutyryl)-α-L-arabinopyranosyl]-22-O-acetyl barringtogenol C)

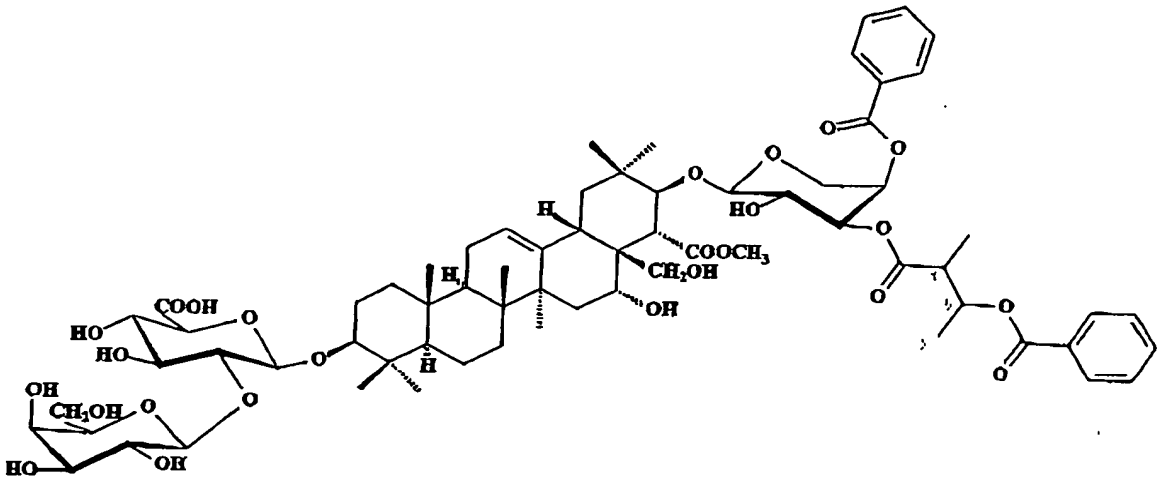

FIG 63 - Compound F70.3.7.2
(3-O-ß-D-galactopyranosyl(1→2)-ß-D-glucuronopyranosyl-21-O-[3-(3-benzoyl-2-methylbutyryl)-4-benzoyl-α-L-arabinopyranosyl]-22-O-acetyl barringtogenol C)

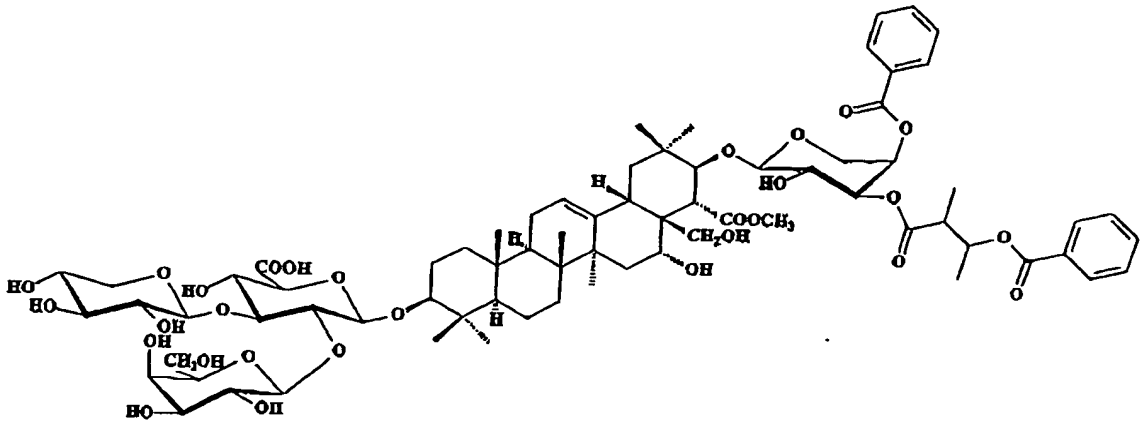

FIG 64 - Compound F80.4.5.2/F80.5.2
(3-O-ß-D-xylopyranosyl(1→3)-[ß-D-galactopyranosyl(1→2)]-ß-D-glucuronopyranosyl-21-O-[3-(3-benzoyl-2-methylbutyryl)-4-benzoyl-α-L-arabinopyranosyl]-28-O-acetyl barringtogenol C)

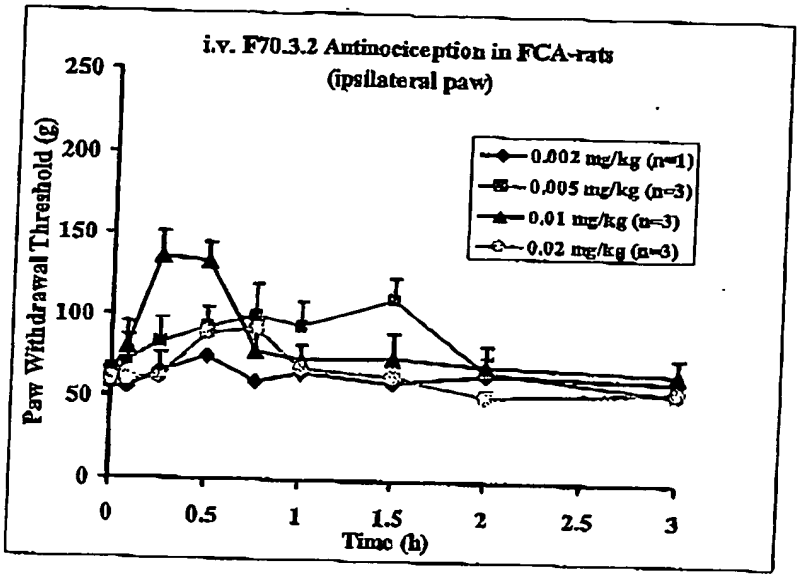

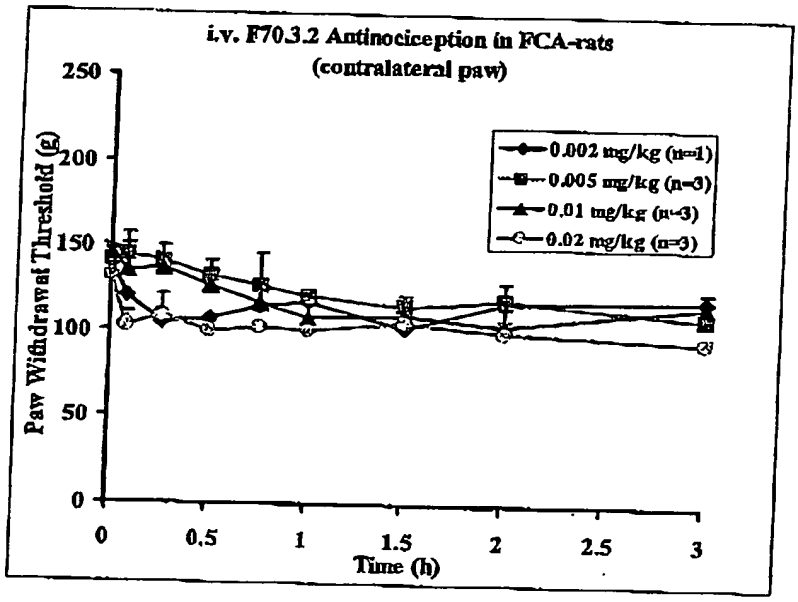

FIG. 65 is a graph of the mean (± SEM) paw withdrawal threshold versus time curves for (A) ipsilateral (inflamed) and (B) contralateral (non-inflamed) hindpaws of FCA-rats.

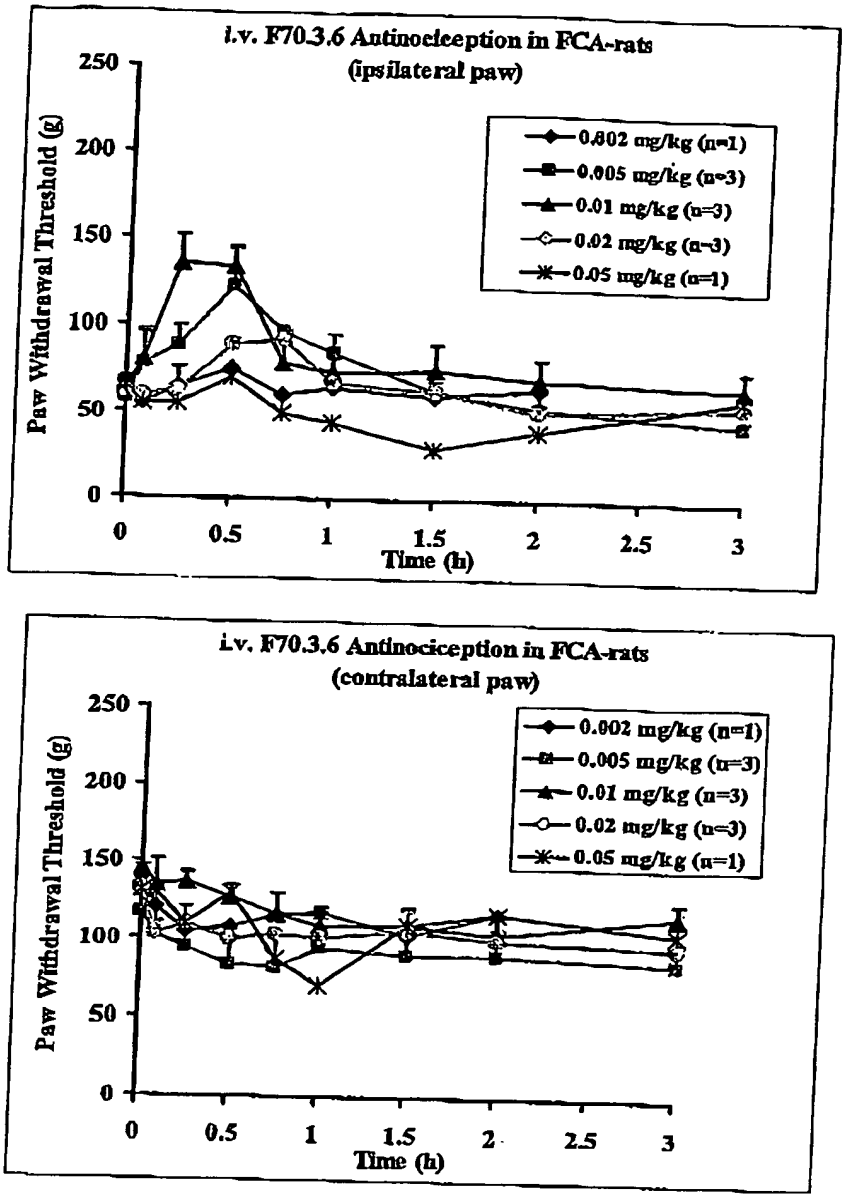

FIG. 66 is a graph of the mean (± SEM) paw withdrawal threshold versus time curves for the (A) ipsilateral (inflamed) and the (B) contralateral (non-inflamed) hindpaws of FCA-rats.

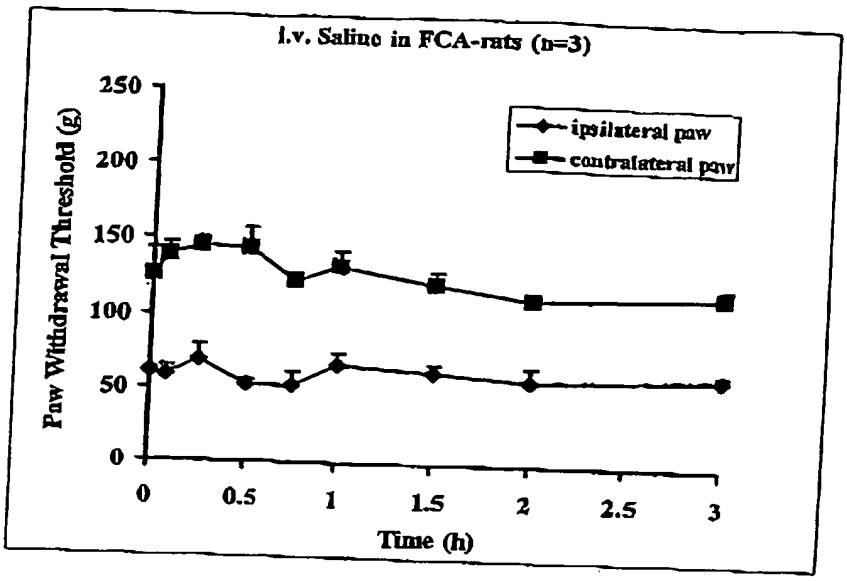

FIG. 67: is the mean (± SEM) paw withdrawal threshold versus time curve for the Ipsilateral (inflamed) and the contralateral (non-inflamed) hindpaw in FCA-treated adult male Sprague-Dawley rats (n = 3) that received a single i.v. bolus of saline.

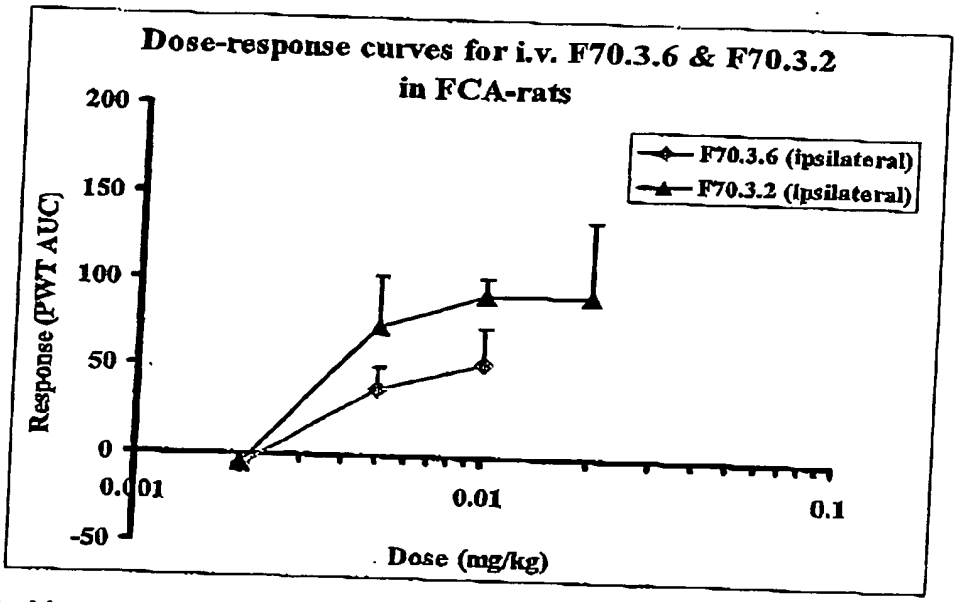

FIG. 68: Mean (± SEM) dose-response curves for the antinociceptive effects of i.v. bolus doses of F70.3.2 and F70.3.6 in the ipsilateral hindpaws of FCA-rats.

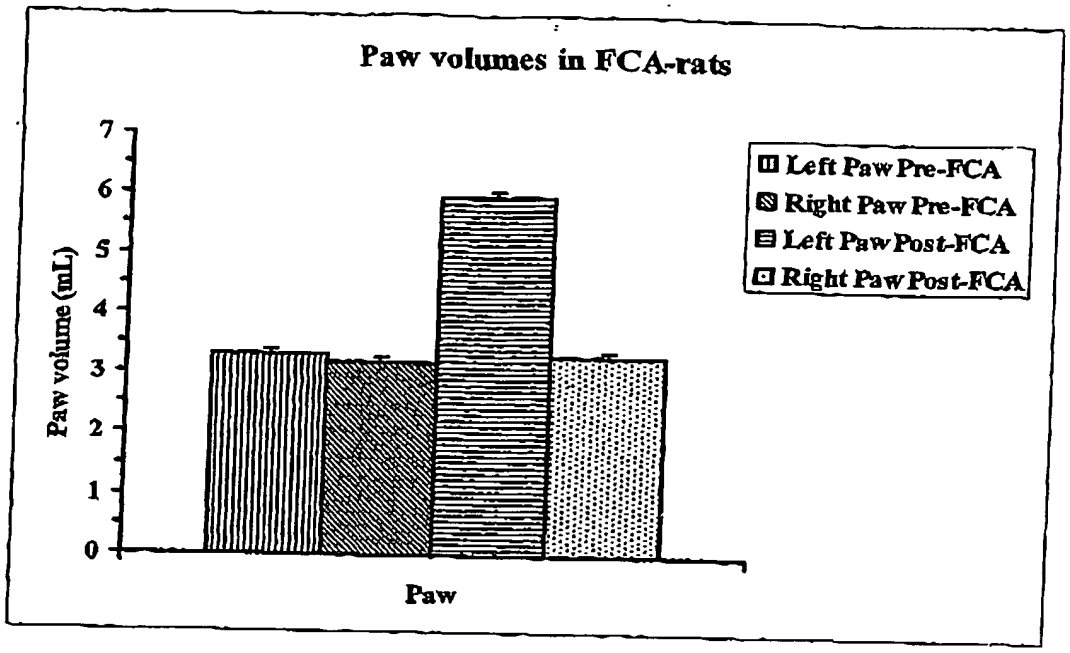

FIG. 69 Is a graph of the paw volume pre and post FCA treatment.